UNIVERSITY OF CALIFORNIA

Los Angeles

A Comparison Study of JPRESS and COSY for Quantitation of 2D Magnetic Resonance Spectroscopy

A thesis submitted in partial satisfaction

of the requirements for the degree Master of Science

in Biomedical Engineering

by

Enrique Frias Martinez

2008

The thesis of Enrique Frias Martinez is approved.

Alex A.T. Bui

Warren Grundfest

M. Albert Thomas, Committee Chair

University of California, Los Angeles

2008

TABLE OF CONTENTS

LIST OF FIGURES

LIST OF TABLES

LIST OF ABBREVIATIONS

2D	Two Dimensional
1D	One Dimensional
Ala	Alanine
Asc	Ascorbic Acid
Asp	Aspartate
Cho	Choline
COSY	Localized Shift Correlated Spectroscopy
Cr	Creatine
Cr303	Creatine Singlet a 3.03ppm
Cr39	Creatine Singlet at 3.9ppm
CRLB	Cramer-Rao Lower Bound
FFT	Fast Fourier Transform
FID	Free Induction Decay
GABA	γ- aminobutyric acid
Glc	Glucose
Gln	Glutamine
Glu	Glutamate
Glx	Gln+Glu
Gly	Glycine
GPC	Glycerophosphorylcholine

GSH	Glutathione
JPRESS	J-resolved Spectroscopy
Lac	Lactate
mI	myo-Inositol
MR	Magnetic Resonance
MRS	Magnetic Resonance Spectroscopy
NAA	N-Acetylaspartate
NAAG	N-acetylaspartylglutamate
PCh	Phosphorylcholine
PE	Phosphorylethanolamine
ppm	Parts per million
PRESS	Point-resolved spectroscopy
ProFit	Prior-Knowledge Fitting
ROI	Region of Interest
ROI	Region of Interest
Scy	Scyllo-inositol
SD	Standard Deviation
SNR	Signal to Noise Ratio
T	Tesla
Tau	Taurine
t-Cho	Total Choline, GPC+PCh+Cho
t-NAA	NAA+NAAG

ACKNOWLEDGEMENTS

I would like to express my gratitude to my advisor, Professor M. Albert Thomas, for introducing me to a new and exciting field such as multi-dimensional MR spectroscopic quantitation and for teaching me invaluable lessons on the workings of research. Without his ability to identify interesting research problems and his vision for the role of spectroscopy in clinical applications, this thesis would not exist.

I would also like to thank the members of my Thesis committee, Professors Warren Grundfest and Alex Bui for their comments and contribution to the final version of this dissertation.

Last but not least, I wish to give a special thanks to all the people in professor's Thomas lab: Rajakumar, Sherry, Scott, Shida, Aparna and Gaurav with which I have closely worked during the last year.

ABSTRACT OF THE THESIS

A Comparison Study of JPRESS and COSY for

Quantitation of 2D Magnetic Resonance Spectroscopy

by

Enrique Frias Martinez

Master of Science in Biomedical Engineering

University of California, Los Angeles, 2008

Professor M. Albert Thomas, Chair

Magnetic Resonance Spectroscopy (MRS) enables non-invasive recording of metabolite concentrations in human tissues. Traditionally, metabolite concentrations have been obtained directly by integrating the area under the curve of a given peak in 1D spectroscopy. The main limitations of such approach were due to the dependence from the operator and his/her ability to identify the metabolite peaks. Fitting algorithms such as LC-Model, J-MRUI, etc. have been developed for automatically obtaining metabolite concentrations form the spectral data. Even though these algorithms overcome the limitations of manual approaches, there are limitations imposed by 1D spectroscopy,

mainly due to the overlap of different metabolite peaks. From a quantitation perspective, this fact limits the specificity and the accuracy of the possible results. A possible solution to this limitation is to increase the magnetic field strength (B_0) of the scanner in order to improve the spectral dispersion of different metabolite peaks.

Another remedy for overcoming the specificity limitation is the use of multidimensional spectroscopy. In 2D MR Spectroscopy, the added dimension facilitates the separation of overlapping metabolites thus increasing the overall accuracy of results. Development of 2D fitting algorithms is still an open research problem but there are some algorithms, such as ProFit, that have been developed recently for a particular 2D MRS sequence, namely JPRESS.

This thesis presents a study to measure the impact of some factors on the quality and accuracy of the measurement of metabolite concentrations using MR spectroscopy: (1) the influence of the magnetic field, (2) the influence of going from 1D spectroscopy to 2D spectroscopy and (3) the influence of using two different 2D sequences, namely COSY and JPRESS, that offer different spectral dispersion of metabolites.

The results presented indicate that: (1) as expected, an increase in magnetic field implies an increase in the specificity and detectability of metabolites; (2) an increase of the dimensionality implies also an increase in the specificity and detectability of metabolites; and (3) when using different 2D sequences, the sequence that offers more spectral dispersion provides better metabolite quantitation, i.e. COSY outperforms JPRESS.

CHAPTER 1

INTRODUCTION

For the last twenty years Magnetic Resonance Spectroscopy (MRS) has been used as a reliable non invasive tool for biochemical investigations of human tissues. Major research efforts in this area have focused on a) optimization of acquisition techniques from well defined localized regions, and b) development of algorithms for obtaining the absolute or relative concentration of metabolites from the MRS signals, i.e. quantitation algorithms.

Although some of the clinical potentials of MRS have been recognized more than a decade ago, it has not completely reached the clinical setting, mainly because of the complexity of the process, and the difficulty of working with data represented in the frequency domain. MRS clinical research areas have focused mainly in human brain, prostate and breast. The typical research approach consists on characterizing a given pathology (for example, depression in the brain, or cancer in the prostate) by measuring the changes in metabolite concentrations between healthy and non-healthy individuals. In order to be able to efficiently implement this approach it is needed a technique that, from the MRS signal, and without the intervention of an operator, automatically obtains the concentration of the relevant metabolites.

MR spectroscopic quantitation can be defined as a mathematical process that having the measured MRS signal as input, obtains numerical values that characterize each one of the components (metabolites) of a spectroscopic signal [39]. This is in general a very

complex task because of the complexity and overcrowded spectra of in-vivo tissue and because of the unpredictable forms of the line shape and baseline.

There are two main approaches for measuring the concentration of metabolites of a MRS signal: (1) using the time domain signal and (2) using the frequency domain signal. Although it may seem more natural to process the signal in the time domain, just because it is its original form, frequency domain processing has produced very good results. These approaches can also be classified depending on whether they use or not use prior knowledge. In this context prior knowledge is defined as any knowledge regarding the metabolites that are part of the spectrum to be fitted. Many studies using time as well as frequency domain data have shown that the inclusion of prior knowledge is essential for reliable quantification [39].

When talking about MRS it is typically understood that the focus is 1D MRS. A wide variety of sequences have been designed, but in general point-resolved spectroscopy (PRESS) can be considered the standard. PRESS [5] is a multi echo single shot technique to obtain spectral data that uses a 90°-180°-180° (slice selective pulses) sequence. The 90° RF pulse rotates the spins in the yx-plane, followed by the first 180° pulse and the second 180° pulse, which gives the signal. With the long echo times used in PRESS, there is a better visualization of metabolites with longer relaxation times. Nevertheless, 1D MRS has significant limitations, mainly the overlap of peaks corresponding to different metabolites. From a quantitation perspective, this fact limits the accuracy of the possible results. One of the possible solutions is to use higher

magnetic fields. Although there are experimental scanners that work at 9T and above, those have still not been approved for humans.

A powerful approach to increase specificity in MRS signal and indirectly increase the accuracy of quantitation algorithms is the use of multidimensional spectroscopy [26]. In two-dimensional (2D) MRS and additional spectral dimension (indirect dimension) facilitates the separation of overlapping multiplets. These indirect dimensions are encoded by varying lengths of evolution periods. The increased specificity that multidimensional spectroscopy provides implies an increase in the accuracy of the concentrations obtained. Typically, up to now, the efforts in multidimensional spectroscopy have been in 2D with sequences such as JPRESS (J-resolved Spectroscopy) [26][34] and L-COSY (Localized Shift Correlated Spectroscopy) [34].

1.1 Two Dimensional MR Spectroscopy: JPRESS & COSY

Two dimensional MRS and its multi-dimensional derivatives have revolutionized the applications of MR to biological macromolecules. Although earlier implementations of multidimensional spectroscopy were initially inefficient due to hardware limitations, as of today, both JPRESS and COSY are well established 2D techniques [34].

In general, in a 2D NMR spectrum acquisition, a 1D sequence is repeated with the evolution period (t_1) incremented in small steps. As the cross peaks are spread onto a 2D plane connecting the resonance frequencies of both J-coupled partners, many metabolite peaks overlapping in a 1D spectrum can be resolved clearly. In addition, a 2D spectrum

has a diagonal which contains signals from the uncoupled spins as well as other coupled spins, much like a 1D spectrum [9].

Localized two-dimensional *J*-resolved spectroscopy (*J*PRESS) is a simple spin-echo experiment with different echo times encoding the *J* coupling in the indirect t_1 dimension consisting of three slice-selective RF pulses (90°-180°-180°). The echo top is used as reference point for the reconstruction along t_1 so that no chemical shift (CS) evolution is present in that dimension. The *J* evolution is not influenced by the 180° pulses and is hence resolved along t_1. The acquisition is encoded along the direct t_2 dimension, which contains both CS and *J* evolution. After a Fourier transformation of the data in two dimensions, a spectrum is obtained with its resonances aligned on the horizontal (0 Hz) axis. *J*-coupled spin systems are split up into multiplets tilted by 45 degrees. As a result the original 1D resonance lines are better separated. The dispersion of metabolites when using JPRESS is defined by -20Hz and +20Hz in t_1. JPRESS has been applied to human brain [15], muscle [16], prostate [44] and breast [4].

Although JPRESS is able to separate J-coupled metabolite resonances, there are still complex 2D cross-peaks patterns for some metabolites [36]. Compared to JPRESS, an L-COSY spectrum produces a better dispersion of J-cross peaks. The L-COSY sequence typically consists of three slice-selective RF pulses (90°-180°-90°) for the volume localization and the last 90° RF pulse also enables the coherence transfer necessary for correlating the metabolite peaks in the second dimension. The dispersion of metabolites when using COSY is much wider that when using JPRESS and comprises and area

defined approximately by -150Hz and +150Hz in t_1. COSY has already been used to brain [3], prostate [33] and breast [32].

Figure 1 and 2 present the pulse sequences for JPRESS and L-COSY. Figure 3 presents a typical 1D PRESS spectrum at 3T, Figure 4 a typical 2D JPRESS spectrum at 3T, while Figure 5 presents a typical 2D L-COSY spectrum at 3T.

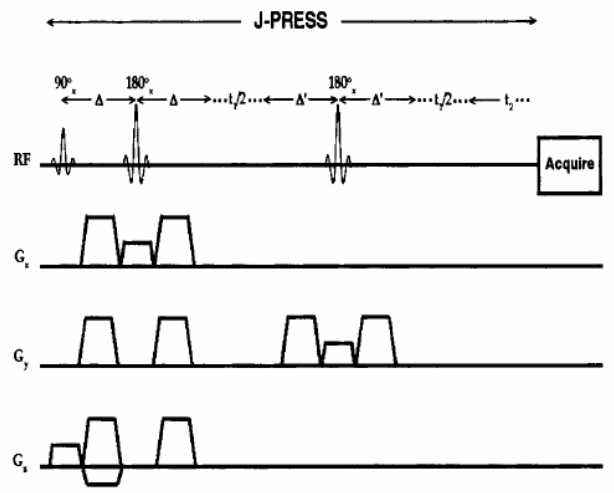

Figure 1. Pulse sequence for 2D JPRESS.

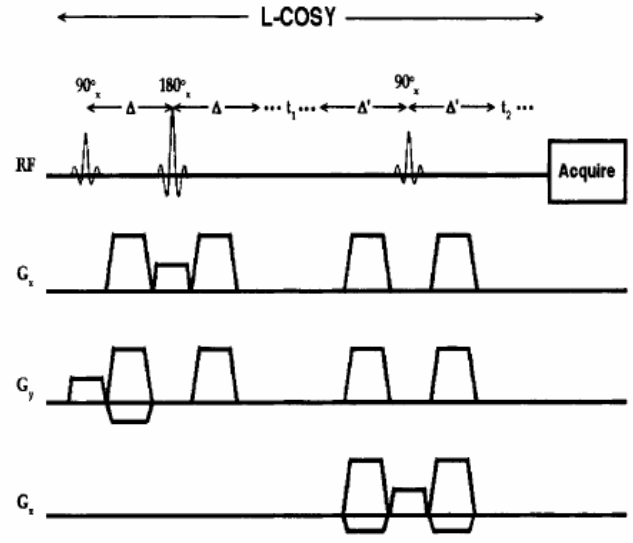

Figure 2. Pulse sequence for 2D L-COSY.

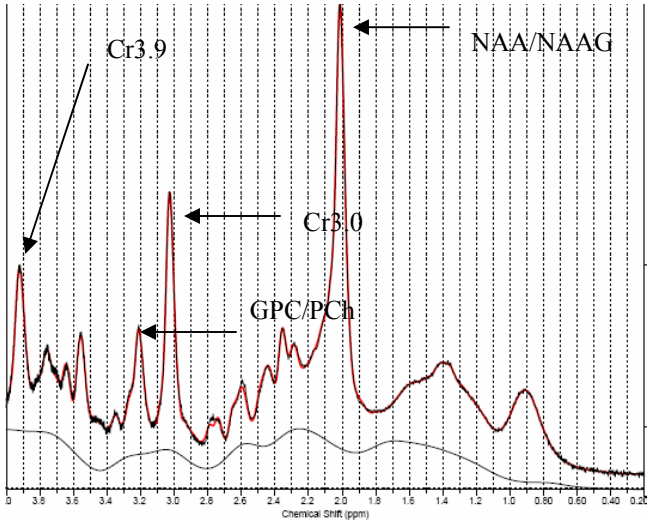

Figure 3. Typical 1D PRESS spectrum acquired at 3T.

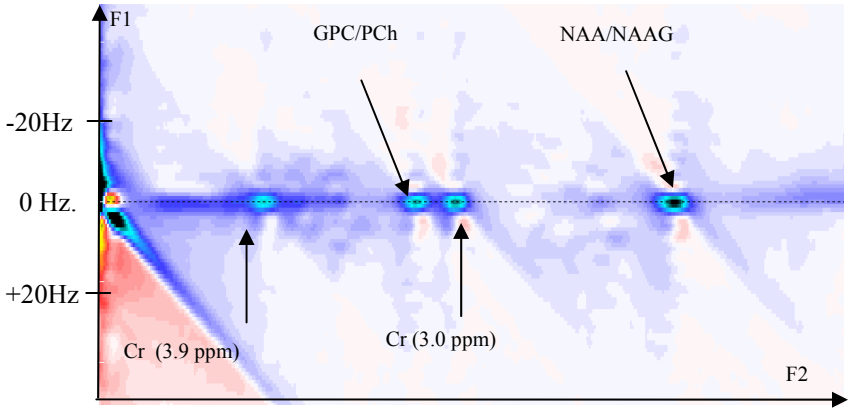

Figure 4. Typical 2D JPRESS spectrum acquired at 3T.

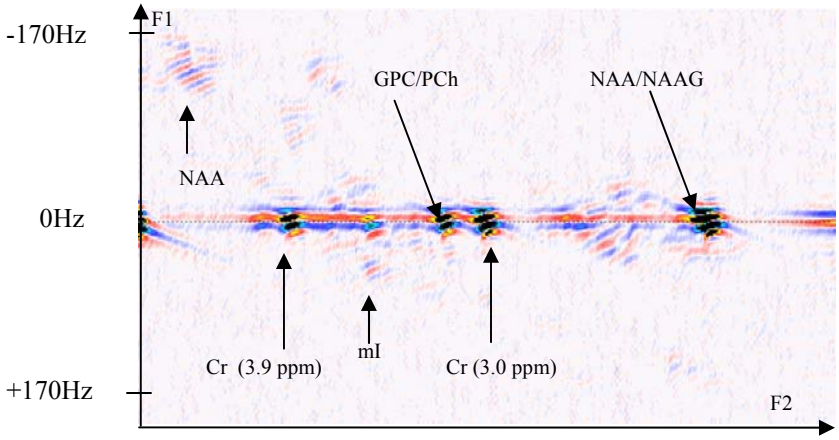

Figure 5. Typical 2D L-COSY spectrum acquired at 3T.

As evident in Figures 4 and 5, 2D spectra have more information on the metabolites that 1D spectrum because of the added information captured by the second dimension. The comparison between JPRESS and COSY highlights the fact that COSY spreads the cross peaks further apart, thus reducing the ambiguity of metabolites and increasing the metabolite specificity.

The assumption behind using 2D MRS as compared to 1D MRS is that better disentangling of the metabolites will imply a better accuracy of quantitation results. Following the same idea, COSY should provide better results than JPRESS. There are other parameters which have a direct impact in the quality of the measurements, mainly the magnetic field of the scanner.

It has to be noted that, strictly speaking, the problem of quantitation is independent from the sequence used in the scanner to capture the signal. Nevertheless, in order to calculate the concentration of the metabolites two elements are influenced by the scanner sequence: (1) because the first step is to reconstruct the MRS signal, the parameters of the sequence used to generate the signal are needed and (2) if needed, prior knowledge should be generated according to the sequence used.

1.2 Objectives and Organization

The generic goal of this thesis is to provide tools that facilitate the use of MRS spectroscopy for clinical applications. Following this idea, this thesis adapts and studies the influence of different factors in 2D MRS spectroscopy quantitation.

The main objectives of this thesis are:

- Modify existing 2D quantitation algorithms for processing the data produced by the UCLA Radiology MRI scanners.
- Study the effects of different magnetic fields for quantitation purposes. The assumption to be tested is that higher magnetic fields will increase the accuracy of the measurements.
- Study the effects of disentangling overlapping *J* coupled metabolite resonances for quantitation purposes. The assumptions here are: (1) 2D spectroscopy will provide better accuracy that 1D spectroscopy and (2) COSY will provide better accuracy that JPRESS.
- Give an example of how quantitation of metabolites can be used for clinical applications.

The following chapter will introduce the basic concepts and algorithms for quantitation of metabolites using 1D and 2D MR spectroscopy signals. This chapter will present in detail the algorithms that will be modified in the latter chapters. Chapter 3 presents a detailed study of the measurements obtained at different magnetic fields and between 1D and 2D signals. The following chapter presents a similar study but comparing COSY with JPRESS. Chapter 5 presents a clinical application of cerebral metabolite quantitation for characterizing late life depression patients and Chapter 6 finishes with the conclusions and future works.

CHAPTER 2

QUANTITATION OF 1D AND 2D MR SPECTROSCOPY

The goal of this chapter is to introduce the basic concepts and algorithms behind the metabolite quantitation of MR spectroscopic signals. The first section introduces the basic spectroscopy signals definitions and details the information relevant for metabolite quantitation. The following sections detail algorithms for 1D as well as 2D quantitation. The last section describes a technique for measuring the quality of the results, Cramer-Rao Lower Bounds (CRLB).

2.1 1D & 2D Spectroscopy Signal and its Information Content

Any MR spectroscopy sequence produces as output a signal called FID (Free Induction Decay) that contains oscillations function of time combined with some noise. The FID is typically expressed as a sum of exponentially decaying sinusoids. This information is obtained from a single volume or voxel localized by programming a localization sequence in the scanner. Once the voxel has been identified, the acquisition process starts immediately, in which consecutive pulses obtain the MRS signal of the voxel. The second (indirect) dimension, which encodes the *J* coupling of the metabolites, is generated with different sampling times. The model function used to represent the FID signal is usually [40]:

$$y_n = \overline{y_n} + e_n = \sum_{k=1}^{K} a_k e^{j\phi_k} e^{(-d_k + j2\pi f_k)t_n} + e_n, n = 0,1,...N-1, \qquad (1)$$

where K represents the number of different resonance frequencies and j=√-1. The parameter a_k represents the amplitude, which is proportional to the number of nuclei contributing to the spectral component with frequency f_k. The damping d_k provides information about the mobility and macromolecular environment of the nucleus. The parameter t_n represents the sampling time point, which can also be expressed as:

$$t_n = n\Delta t + t_0 . \qquad (2)$$

Typically the acquisition starts after a time delay (usually half echo time) t_0. The imaginary part of the second exponent is usually called the zero-order phase. The factor e_n represents the noise and is assumed to be complex and Gaussian.

The time representation of the signal can not be used to visually identify its components, so a fast Fourier transform (FFT) is typically used for better representing the information. Applying FFT to this time domain signal leads to a frequency domain spectrum consisting in a sum of Lorentzian lines. While in 1D spectroscopy, a Fourier transform is needed only once, in 2D spectroscopy two Fourier transforms are needed, one for each dimension. Figure 6 presents an example of how a 2D MRS signal acquired using a JPRESS sequence looks after double Fourier transform in each dimension. The figure on the left basically shows how the water peak dominates the whole spectrum, while the figure on the right shows how the metabolite peaks can be observed if the water peak is filtered. By selecting the area in which the metabolite peaks are present the problem of quantitation is easier to solve. In quantitation algorithms this area is typically

called Region of Interest (ROI). Figure 7 presents how the ROIs typically look in 2D (left) and 1D (right).

Using the concept of ROI, the problem of quantitation of an MRS signal can be simplified, and expressed as identifying the concentration of metabolites only from the selected region of the spectrum. Although identifying this region is a very useful approach when using frequency techniques, in time domain the same concept tends to be more complex and not as useful.

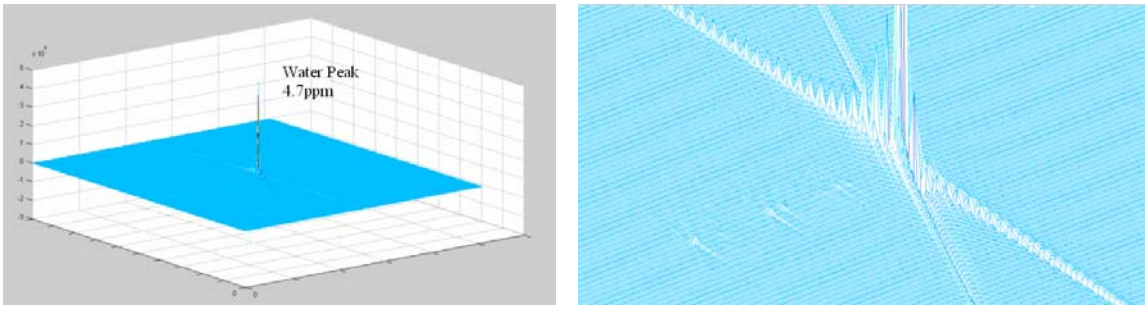

(a) (b)

Figure 6. (a) Double FFT of 2D JPRESS raw data and (b) metabolite peaks in that signal.

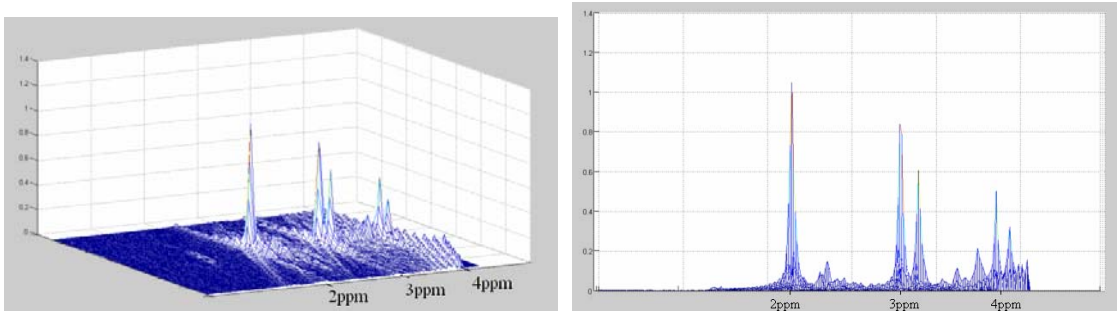

(a) (b)

Figure 7. (a) Area that contains the relevant information in 2D and (b) Representation of the relevant area for a 1D signal.

The individual signals produced by each metabolite are summarized by the final signal produced by the scanner. These individual signals are characterized by a set of factors: (1) resonance frequency, (2) line shape, (3) line width, (4) phase and (5) amplitude. Each

metabolite has a predefined set of values for these factors. From these set of factors, resonance frequency and amplitude are the ones that contain the most relevant information because they identify the metabolite and give an indication of the concentration. The other factors, although not relevant for quantitation, need to be determined to correctly identify the amplitude of each component.

Resonance Frequency

The resonance frequency is used to identify the biochemical elements that compose each one of the metabolites considered. These shifts, at least under standard situations, are considered constant. For example, Cr has two peaks, one at 3.03ppm and another at 3.9ppm, NAA and NAAG both have one peak at 2ppm, and GPC has one peak at 3.2 ppm. However the relative spectral position can be affected by external parameters like pH or temperature, i.e. the theoretical position can be slightly shifted in a real environment. This possibility has to be considered when using automatic techniques for identifying each one of the peaks in order to quantify them. Fig 8(a) presents a 1D example of the ppm in which the most important metabolites appear, while Fig. 8(b) presents the same information but for a 2D JPRESS spectrum.

Signal Amplitude

This is the most important parameter for quantitation. The analysis of amplitudes reflects the concentrations of the metabolites due to the fact that the amplitude is proportional to the concentration of the corresponding molecule. When analyzing this information it has to be considered that the volumes selected for obtaining the MRS signal can contain a variety of elements (blood vessels, intercellular spaces, etc.), and

even if those elements are not included, the volume of interest will usually contain thousands of cells with different levels of homogeneity. In general these factors are not considered and the homogeneity of the cells described by the MRS signal is assumed. Amplitude is the key element for the clinical applications of MR spectroscopy because it provides a marker and a signature for a specific pathology.

Line width, Phase and Line shape

The line width (or dampening) reflects the dynamical magnetic environment of the molecule. The phase reveals finer interactions between spins of the same molecule. In general the line shape of the molecules, considering an ideal situation in which they are freely and homogeneously distributed in water, will be Lorentzian. Nevertheless pure Lorentzian shape is never observed in real MR spectroscopy signals due to variations in the magnetic fields or different susceptibilities of the tissue.

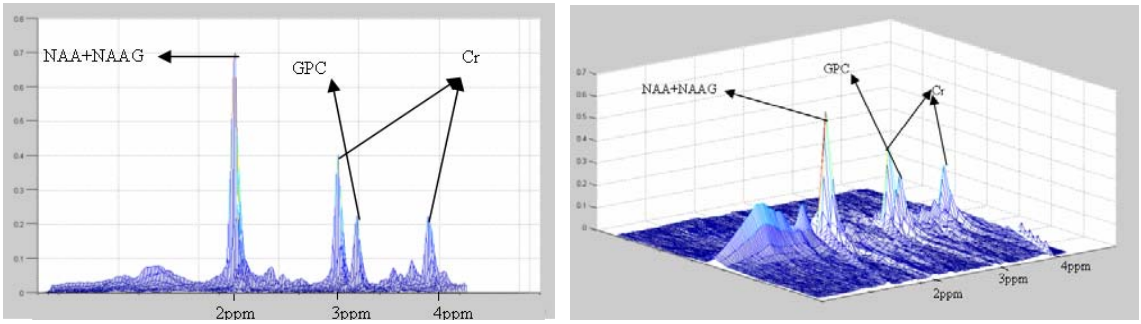

(a) (b)

Fig. 8. (a) Identification of metabolites in a 1D PRESS signal and (b) in a 2D JPRESS signal.

2.2 Basic Preprocessing of MRS signals

The condition in which MRS signal acquisition is done usually produces distorted signals not directly suitable for analysis. Quantitation results can be improved using preprocessing algorithms to eliminate or correct data imperfections. Although

quantification techniques can be very different in their approaches, there is a common set of tools used for preprocessing the original MRS signal [45].

Zero-filling

Zero-filling or zero-padding consists on extending the number of sampled time domain points of zero amplitude with the aim of obtaining an improved digital resolution for a better spectral visualization [2]. This technique can be done both in frequency and time domains.

Filtering

To visually improve the signal-to-noise ratio (SNR) and/or the resolution of the acquired spectrum, the FID can be filtered by a function in the time domain. By multiplication with a decreasing exponential, the noisy data points at the end of the FID are attenuated and the width of the peaks in the spectrum increases, resulting in a spectrum that looks less noisy. There are a wide variety of filters, although typically a Gaussian filter is used. For a 1 D spectrum a Gaussian filter is defined as:

$$G(x) = \frac{1}{\sqrt{2\pi}\sigma} e^{-\frac{x^2}{2\sigma^2}}, \qquad (3)$$

with σ defined as the standard deviation of the noise.

Referencing to a Signal

Although this type of preprocessing is not as common as the previous two it is useful when there has been a shift in frequency that complicates the identification of the components of the signal. The basic idea is to use the water peak, which is the stronger signal, to reposition the rest of the peaks considering water as a reference. This approach

allows to identify the rest of the peaks in situations where the signal-to-noise ratio is low or where the shift in frequency makes it difficult to identify each metabolite. When using the latest quantitation techniques, there is no need to use water in order to reference the rest of the signal because these techniques already consider the possible shifts of the peaks in order to obtain the best fit.

Baseline Correction

The baseline of the signal obtained from applying the Fourier transform will reflect not only the metabolites of the selected volume, but also noise, experimental artifacts and the resonance of large molecules such as lipids. All these elements will affect the quantitation of the metabolites, especially of the metabolites with smaller concentrations, because their peaks could be buried by those elements. It is then very important to have mechanisms to correct this background signal. There are different techniques for estimating the baseline based on splines or polynomial functions [23]. Fig. 9 presents two examples where baseline correction is needed because (a) presence of lipids and (b) poor water suppression.

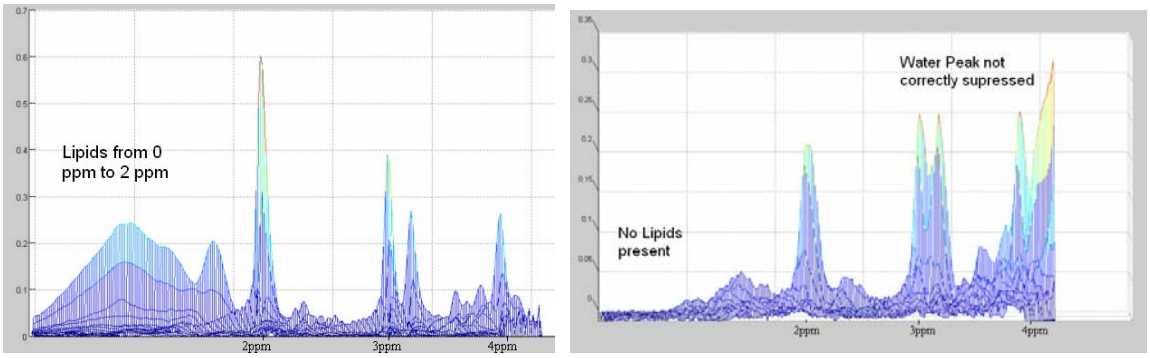

(a) (b)

Figure 9. Example of required baseline correction caused by (a) lipid contamination and (b) poor water suppression.

2.3 Algorithms for Quantitation of 1D MR Spectroscopy

The quantitation process can be done using the MRS signal expressed in the time domain or expressed in the frequency domain. This section details different solutions that have been designed using each one of these approaches. Any of the methods used is based on some previous knowledge of the metabolite for which the concentration is going to be obtained, typically the resonance frequency. This prior knowledge is a key element to implement quantitation because it somehow equilibrates the intrinsic low signal-to-noise ratio and overlap of peaks that are typical of MRS signals [30][37]. The results that these approaches provide are not absolute concentrations but in general a ratio of concentrations considering as a reference one of the metabolites. For example, in brain MRS, concentrations are usually expressed as a ratio to the concentration of creatine (Cr).

2.3.1 Algorithms for Quantitation in Time Domain

Although there is a wide variety of different time domain methods the best part of them can be grouped under what are usually called interactive methods [21]. The goal of an interactive quantitation method is to minimize the function:

$$\left\| \mathbf{y} - \mathbf{y}' \right\|^2 , \qquad (4)$$

where $\mathbf{y}=[y_0 \ldots y_{N-1}]^T$, is the original FID signal, $\mathbf{y}'$ is the approximated signal, and $\| \cdot \|$ is the Euclidean vector norm. This problem is typically solved using non-linear least-squares techniques. The problem can be simplified by dividing it into a linear and a non-linear part by rewriting the function (1) as:

$$y_n = \sum_{k=1}^{K} c_k \gamma_k(\alpha_k, n), n = 0,1,...N-1, \quad (5)$$

where K represents the number of different resonance frequencies, c_k represents the complex amplitude and the $\gamma_k(\alpha_k,n)$ are independent functions of the nonlinear parameter vector α_k. Following the equation (1) α_k is a function of $[f_k\ d_k\ t_0]$,

$$c_k = a_k e^{j\phi_k}, \quad (6)$$

$$\gamma_k(\alpha_k, n) = e^{(-d_k + j2\pi f_k)t_n}. \quad (7)$$

Rewriting (5) as a matrix:

$$\bar{\mathbf{y}} = \mathbf{\Gamma c}, \quad (8)$$

With,

$$\mathbf{c} = [c_1, ..., c_k]^T, \quad (9)$$

$$\mathbf{\Gamma} = \begin{bmatrix} \gamma_1(\alpha_1, 0).....\gamma_K(\alpha_K, 0) \\ ..... \\ \gamma_K(\alpha_K, N-1).....\gamma_K(\alpha_K, N-1) \end{bmatrix}, \quad (10)$$

If the non-linear parameters α_k are known, then the matrix $\mathbf{\Gamma}$ can be computed and an estimate for the linear parameters $\mathbf{c}$ is obtained as the solution of a linear problem:

$$\mathbf{c} = \mathbf{\Gamma}^m \mathbf{y}, \quad (11)$$

where $\mathbf{\Gamma^m}$ denotes the pseudo inverse of a (non-squared) matrix. After that the cost function expressed in (4) can be rewritten as:

$$\left\| \mathbf{y} - \mathbf{\Gamma\Gamma}^m \mathbf{y} \right\|^2, \quad (12)$$

which is a cost function that contains only non-linear parameters and thus can be solved using non-linear programming techniques.

The main problem that these types of algorithms have is that $[f_k\ d_k\ t_0]$ have to be known, or at least an approximation, in order to start the algorithm. This implies that a lot of interaction is needed from the users, thus the name interactive methods. Recently algorithms to automatically approximate these values from the spectrum have been developed. These approximations facilitate the application of local methods (such as the linear and non-linear minimization) that highly depend on the initialization values. Nevertheless no methods exists that guarantees convergence to the local minimum in a reasonable amount of time. Another possible solution consists on using global optimization procedures, such as genetic algorithms [19, 42]. In this case there is no need to have a good initialization of the parameters but the inconvenient is that they have poor computationally efficiency.

There are a variety of algorithms that use this general idea and that differ in the non-linear programming technique that they use, like VARPRO [38] or AMARES (Advanced Method for Accurate Robust and Efficient Spectral Fitting) [41] that improves VARPRO in terms of robustness and flexibility, both part of the MRUI [14] (Magnetic Resonance User Interface) package.

2.3.2 Algorithms for Quantitation in Frequency Domain

The simplest approach for quantitation in the frequency domain is the integration of the areas of a given peak [20]. This approach uses the prior knowledge given by the resonance frequencies of each metabolite and the experience and knowledge of the

operator that manually selects the limits of the area. This approach has obvious problems: (1) the bias of the operator and (2) the extreme overlap that some metabolites have. Surprisingly, direct integration of the area of a peak is still being used although the results they produce are highly questionable.

A more advanced set of techniques are based on optimization methods. These approaches, to a large extent, solve the problems that the integration approach has: (1) it is an automatic process so there is no bias introduced by the operator, and (2) the use of prior knowledge solves to some extent the problems arising from the overlapping of peaks. The basic idea of this approach is to obtain a linear combination of the prior knowledge of the metabolites represented using their Lorentzian shapes in the frequency domain that better approximates the original signal. Fig. 10, reproduced from [23], presents an example of the prior knowledge (presented in the bottom four rows) and how this knowledge has to be linearly combined to obtain the final signal (top row).

The simple form of the problem is solved by using a linear optimization, such as linear least squares, between the original spectrum and the prior knowledge spectra. Formally:

$$\mathbf{y} = \mathbf{\Gamma c} \Rightarrow \mathbf{c} = \mathbf{\Gamma}^{m}\mathbf{y}\,, \qquad (13)$$

with, $\mathbf{y}$ the original signal expressed in the frequency domain, $\mathbf{\Gamma}$ a matrix that contains the prior knowledge of the metabolites in the frequency domain, $\mathbf{c}$ a vector that indicates the concentration for each metabolite and $\mathbf{\Gamma^m}$ representing a pseudo inverse of a (non-squared) matrix

In general, such solutions only work under ideal situations because do not consider the possible shifts in frequency of the different metabolites peaks. This implies that for a

generic case, a non-linear approach is also needed in order to obtain the frequency shift of each one of the metabolites. In the end, the process of automatic fitting in frequency domain is done using the same algorithm as in time domain but with frequency information. It has to be noted that frequency domain methods that use a Lorentzian model function for the metabolite peaks are in fact totally equivalent to time-domain fitting methods from a theoretical point of view [40]. The main advantage of this approach is that the information can be graphically interpreted.

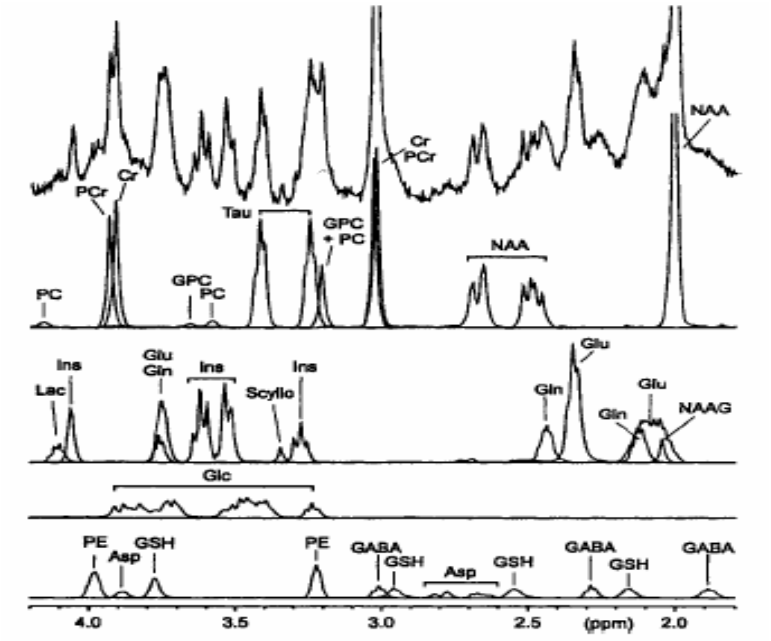

Fig. 10. From top to bottom, (1) original high-quality in vivo spectrum (rat brain at 9.4T) of the region from 1.8 ppm to 4ppm, and (2) last four rows representation of the prior-knowledge of the metabolites used for the fitting.

LC-Model [23, 18] is the most popular algorithm for 1D quantitation in frequency domain, and is typically considered a standard. The algorithm uses a linear combination of the metabolites considered to fit the experimental data in the frequency domain. Because the program does not depend on parameter information of separate peaks but on

the complete spectral pattern of each metabolite, including particular effects of the MR machine over the experiment, it exploits a fairly extensive range of available prior knowledge. This is one of the reasons for the robustness of the algorithm. A non-linear optimization fits the magnitudes, line widths and other parameters of the basis spectra to approximate a measured spectrum. The baseline is modeled by including a spline function into the fit. All the data in the analysis range is simultaneously used in a constrained least squares analysis to obtain approximately maximum-likelihood estimates of all the model parameters (metabolite concentrations, phases, referencing shift, lineshape, etc.). The analysis is automatic and no subjective input from the user is needed. It has been widely used for 1.5T and 3T data for a variety of studies such as epilepsy [25], tumors [8] and Alzheimer's disease [24].

2.3.3 Time Domain Quantitation vs. Frequency Quantitation

Until recently, fitting using time information was considered the best approach. Nevertheless with the introduction of frequency domain techniques based on the generation of prior knowledge, frequency domain techniques have surpassed time domain techniques. In general, in a signal that has baseline problems caused by noise or artifacts, time domains methods will be able to handle the data very efficiently [21]. Frequency domain methods can also deal with this type of data but they will need a preprocessing stage in which the baseline is regenerated. If the baseline does not have any problems, frequency domain methods provide a more attractive solution because they require lower computer requirements and graphical representations are more meaningful. In general for signals with a high signal to noise ratio, both approaches would operate equally well,

although, frequency domain techniques are usually more computationally efficient. Fitting in the frequency domain has a very important advantage over the time domain: that it is very easy to select the region of the spectra to fit, thus eliminating unwanted peaks (mainly water) and possible artifacts of the spectrum.

Apart from the techniques mentioned, the literature presents a wide variety of approaches for quantification of MR signals. Stoyanova and Brown [31] propose the use of PCA (principal component analysis) for simultaneous spectral quantification of a single resonant peak. Antoine et al. [1] present the use wavelets for quantification. Miller et al. [22] uses Expectation Maximization (EM) to reduce the high dimensional search for the optimum parameters of a quantitation model.

2.4 Algorithms for Quantitation of 2D MR Spectroscopy

The basic approach for 2D quantitation is based on the integration of the volume under a given peak. The same problems that present in the 1D approach are also present here but with the added complexity of having to consider a second dimension. Other approaches use 1D techniques applied to a cross section of the 2D spectrum [10, 28]. Efficient quantification of 2D MRS signals is still an open problem and in general current solutions inherit concepts and ideas from 1D quantification algorithm.

2.4.1 Prior Knowledge Fitting Algorithm (ProFit)

More advanced approaches for fitting 1D spectroscopy combine ideas of 1D algorithms using the information in its 2D original form. ProFit [27] (Prior Knowledge Fitting) is probably the most relevant of these algorithms.

ProFit [27] is based on a linear combination of the prior knowledge spectra. The optimization problem consists on identifying the best combination of the basis spectra that minimizes the error when compared with the original spectrum to be fitted. Although the most important parameters to be obtained are the individual concentrations of the metabolites, other intermediate parameters need to be determined as part of the process, like the zero order phase, the shift in f_1 and the Gaussian line broadening. ProFit uses various complementary approaches inherited from previous algorithms: (1) part of the fitting is done in the time domain and part in the frequency domain and (2) part of the fitting is done using a linear approach and part using a non-linear approach. The algorithm can be divided in three main parts: (1) basis set generation (or prior knowledge generation), (2) reconstruction, which is applied both to the basis set and to the data being fitted and (3) fitting of the data using the prior knowledge.

Basis Set Generation

The prior knowledge contains the 2D spectra of each one of the metabolites considered for the study. The spectra are simulated using GAMMA [12, 29] (see next section).

Reconstruction

The signal under analysis is Fourier transformed in two dimensions, time shifted and filtered. The exact filters implemented by the reconstruction process will depend on the sequence used for capturing the spectra (JPRESS, COSY, etc.). After that, and in order to reduce computational time, a region of interest (ROI) that contains the metabolites being studied is obtained from the whole spectra (as done in Figure 3 and Figure 4). The information obtained from this process is stored in a matrix called *S*.

The same process is also applied to each one of the spectral representations of the metabolites of the prior knowledge. The group of matrices obtained from the processing is combined into single matrix *B* that stores all the prior knowledge.

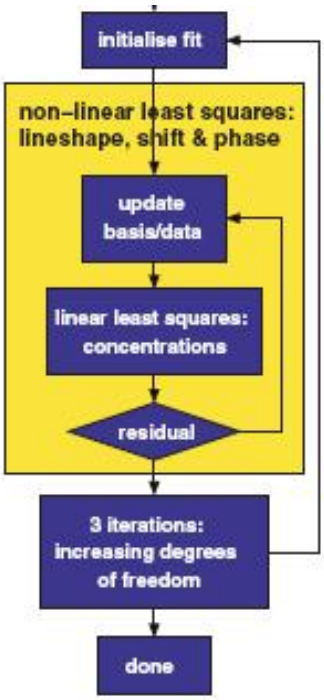

Figure 11. General architecture of ProFit detailing the non-linear optimization (yellow box) and the linear optimization (linear least squares)

Fitting

The fitting algorithm receives as inputs *B*, the matrix that contains a representation of the prior knowledge, and *S,* the matrix that contains the spectral data to be quantitated, and only considers their real part for the process. In order to produce a successful fitting the algorithm is divided into three iterations with increasing degree of freedoms. The first two iterations only consider the most important metabolites (in the case of brain MR signals, creatine, NAA and PCh), while the third one considers all the metabolites of the

prior knowledge. The second and third fits are initialized with the results obtained by the previous iterations. The first iteration is initialized with the zero order phase, the Gaussian line broadening in f_2 and the shift in f_1 obtained from applying algorithms to obtain an approximation from the signal being fitted, *S,* during reconstruction.

The non-linear fitting process is implemented as a gradient-descent algorithm that finds the minimum of a constrained non-linear multivariable function. The constraints express that the concentrations have to be positive. This non-linear optimization uses the data of *B* and *S* expressed in time domain. The objective of the non-linear fitting is to identify the zero order phase, the Gaussian line broadening in f_2 and the shift in f_1 that minimizes the function. The linear part of the process defines the concentrations and the function to be minimized. The concentrations of the metabolites (*C*) are obtained using linear least squares by solving the equation:

$$S = B \cdot C \quad \Rightarrow C = S \cdot Inv(B), \tag{14}$$

where *Inv* represents the Moore-Penrose pseudo inverse (due to the fact that *B* is not a square matrix), and *S*, and *B* are expressed in the frequency domain. The function to be minimized by the non-linear process is defined as:

$$\text{Residual} = S - C \cdot B, \tag{15}$$

Each non-linear optimization implies numerous evaluations of the *Residual* function. After the residual has been obtained the basis spectra parameters (zero order phase, the Gaussian line broadening in f_2 and the shift in f_1) are updated by the non-linear optimization part of the fitting. The non-linear optimization finishes after a predetermined number of iterations or after the gradient reaches a determined value, whichever comes

first. Figure 11, presents how the linear and non-linear parts of the algorithm communicate in order to minimize the residual function and update the non-linear optimization parameters.

2.5 Prior Knowledge Generation

The 1D and 2D algorithms presented are based on some prior knowledge of the spectra. That need is especially important for frequency algorithms that need the spectra of each individual metabolite to be fitted. This prior knowledge is not universal, it will depend on a wide variety of factors, mainly: (1) the strength of the magnetic field, (2) the sequence used in the scanner to obtain the signal, and (3) the set of metabolites for which the concentration is going to be obtained (different clinical studies focus on different metabolites). In order to construct this prior knowledge there are two alternatives: (1) measuring phantom solutions of each metabolite in the scanner and (2) simulation. The main inconvenient of the first alternative is that it is very time consuming because it implies the construction of one phantom for each metabolite and its measurement in the scanner. It may seem that this approach would be ideal for fitting, but in general it has to be considered that the phantom and the scanning would include errors in the prior knowledge. In general, this approach is not used in the literature.

The second approach is typically used for generating prior basis sets, being GAMMA a standard in the field [12]. GAMMA [29] is a C++ library written for simulation of MR resonance experiments by providing the data structures (spins, chemical shifts, coupling, etc.) and operators (Hamiltonians, propagators, density operators, etc.) needed for this

purpose. From the point of view of generating prior knowledge, GAMMA allows to simulate the sequences used in the scanner (PRESS, JPRESS and COSY) and simulate the output that each one of the metabolites will produce. In order to do that, for each one of the metabolites some information is needed: (1) number of spins systems, (2) peak location in ppm of each spin system and (3) *J*-coupling between each pair of spin systems. For the prior knowledge generated for this thesis, the data contained in [13] has been used for metabolite simulation.

2.6 Measuring the Accuracy of a Quantitation

In general, in a clinical environment there are some measurements that cannot be repeated. Because of that, it is not possible to use the standard deviation (SD) as quality of the measurement. This is the case of a MRS signal that is going to be used for quantitation of metabolites, because, if the signal is acquired again: (1) the voxel will not be in the exact same position, (2) the position of the patient will not be the same, (3) the magnetic field would not be exactly the same, etc. If the goal is to use the concentrations of metabolites for clinical applications, obtaining a measurement of the degree of confidence of the concentration obtained is as important as obtaining the estimation of the concentration.

In signal processing, the Cramer-Rao lower bound (CRLB) on the variance of the estimators is typically used as a measure of the attainable precession of parameter estimation from a given set of observations [6, 7]. CRLB express a statistical lower bound for the achievable standard deviation of the estimated parameters:

$$\sigma_{p(l)} \geq CRLB_{p(l)} = \sqrt{(F^{-1})_{ll}} \ . \qquad (16)$$

Typically CRLB are presented as a percentage of the concentration of each metabolite. In general, it is assumed as a standard that concentrations whose CRLB is higher that 20% can not be considered valid [23][27].

CRLB are obtained from the diagonal of the Fisher Information matrix, whose size is equal to the number of parameters being estimated (the number of metabolites in this case). The Fisher matrix expresses the amount of information that an observable variable X carries about another parameter Y. In the case of metabolite concentration, the Fisher matrix can be obtained as [43]:

$$F = \frac{1}{\sigma^2} \mathrm{Re}\{B^{Total}\}^T \, \mathrm{Re}\{B^{Total}\} \ , \qquad (17)$$

where, Re, expresses the real part of the matrix, σ represents the standard deviation of the real part of the noise and B^{Total} represents the total prior knowledge:

$$B^{Total} = \{B_1, B_2, ..., B_m\} \ , \qquad (18)$$

with m the total number of metabolites considered and B_i $i=1,...,m$, the prior knowledge obtained after simulating and reconstructing each metabolite considered. The information that the Fisher matrix contains in this context, is the amount of information that a given metabolite carries from any other metabolite. For example, a metabolite will carry a lot of information about itself (the values of the diagonal would be the predominant ones), two metabolites that have overlapping will have some information about each other, while two metabolite that do not have any overlap will not carry information about each other.

As can be seen, the CRLB of each metabolite does not depend on the concentration of the metabolite, but only on the noise and on the orthogonality of the prior knowledge.

It has to be noted that CRLB is an indication of the quality of the fit, but does not give any indication and is not dependent on the quality of the original data, i.e. CRLB can give very small values but the concentrations could not be valid because the original data was very noisy. ProFit has been designed to provide a measurement of the quality of the original data. The mechanism is implemented by expressing creatine (that has two singlets at 3.9 ppm and 3.03 ppm) as two individual prior knowledge metabolites for which we know that the ratio is, for an ideal signal, one to one. A ratio of Creatine 3.9 compared to Creatine 3.03 smaller than one usually implies a problem with water suppression. Ratios of Creatine 3.9 to Creatine 3.03 bigger than one reflect poor/noisy spectra. ProFit designers suggest that any spectra for which Cre3.9<1.3 should be considered valid [27]. In general, when working with volunteers, the ratio of Cr3.9 is very close to one, so the number of spectra discharged is minimum.

Although this policy is considered valid when working with volunteers, when using it for clinical applications, specially for identifying markers of pathologies, using Cre3.9<1.3 would include as valid data that has been affected by water suppression in the 3.5ppm to 4ppm area. On chapter 5 a deeper discussion of this policy is presented.

CHAPTER 3

QUANTITATION OF 2D JPRESS MR SPECTROSCOPY

The main objective of *in vivo* proton MRS is the determination of individual metabolite concentrations in different human organs. As it was mentioned in the introduction, this can be a difficult task because of the generally complex and overcrowded spectra. There are two main options that can be used to increase metabolite specificity: (1) use higher magnetic fields and (2) multidimensional spectroscopy. The first approach has its limitations, and currently, although there are scanners working at 9T, for human applications, the FDA (Federal Drug Administration) limit is around 3T. The second approach, although increases specificity, is not very popular, mainly because: (1) its complexity, compared to 1D, for implementing the sequences and the postprocessing algorithms and (2) because time, hardware and other constraints only permit the application of the most basic one dimensional sequences such as PRESS and STEAM. In general, the manufacturers of the MRI scanners do not provide JPRESS and L-COSY sequences.

The goal of this chapter is to verify to which extent the two previous approaches increase metabolite specificity: (1) to which extent the increase in the magnetic field used by the scanner increases specificity and (2) to which extent the increase in dimensionality (going from 1D spectroscopy to 2D spectroscopy) increases the overall specificity. The scanners used for testing these assumptions were the following: a 3T Siemens Trio (Siemens Medical Systems, Germany) and a 1.5T Siemens Avanto (Siemens Medical Systems, Germany).

For testing the second assumption, 1D PRESS and 2D JPRESS have been implemented. The JPRESS implementation used for this work is derived from the regular PRESS sequence, where the first echo time (TE_1) is always chosen as short as possible and only the second refocusing pulse is shifted for encoding t_1. The sampling of the second echo signals starts immediately after the signal crusher gradient of the last 180 degrees pulse, as shown in Fig. 1.

The first section details the changes made to ProFit to quantify the metabolites, the second section presents the comparison between 1.5T and 3T quantitation, and the third section compares 1D PRESS with 2D JPRESS quantitation.

3.1 ProFit Modifications for 3T Siemens Trio and 1.5T Siemens Avanto

Although the algorithm in which ProFit is based is independent of the sequence, the platform and the magnetic field it has some parameters that are affected by these values. Originally ProFit was designed for a Philips Intera 3T whole-body scanner (Philips, Best, The Netherlands) so in order to be used for Siemens scanners some changes have been made: (1) reversal of the spectrum (left to right), (2) generation of prior knowledge for JPRESS 3T and 1.5T and (3) calculation of total concentrations and CRLB values for Glx (Gln+Glu), total choline (t-cho=GPC+PCh+Cho) and t-NAA (NAA+NAAG).

Reversal of the Spectrum

Due to design reasons, the way in which a Philips scanner and a Siemens scanner store information is shifted 180 degrees. This caused problems in reconstruction when using the original algorithm. The solution to the problem was to undo the 180 degrees shift present in the Siemens scanner multiplying by -1 the real part of the FID of the spectrum.

Generation of Prior Knowledge for Siemens Trio and Siemens Avanto

Although Siemens Trio is commercialized as a 3T scanner the real value of its magnetic field is 2.89T. This implied that the original prior knowledge that ProFit has, designed for a 3T Philips scanner could not be used. It was also decided to include Choline (Cho) as part of the prior knowledge, which was not part of the ProFit's prior knowledge.

Prior knowledge was generated using a JPRESS simulation using GAMMA [12] with the following parameters: *T=2.89, TR/TE=2.0s/30ms*, 100 $\Delta t1$ increments 2048 points in t_2 and te_1*=14ms*. It was generated for 20 metabolites: creatine (Cr), N-acetylaspartate (NAA), glycerylphosphocholine (GPC), phosphorylcholine (PCh), free choline (Cho), alanine (Ala), aspartate (Asp), γ-aminobutyric acid (GABA), glucose (Glc), glutamine (Gln), glutamate (Glu), glycine (Gly), glutathione (GSH), lactate (Lac), myo-inositol (mI), N-acetylaspartylglutamate (NAAG), phosphoethanolamine (PE), taurine (Tau), scyllo-inositol (Scy) and ascorbate (Asc). Prior knowledge for Creatine was divided in two different files one for each singlet, one for Creatine at 3.03ppm (Cr303), from the N-methyl proton, and another one for creatine 3.9ppm (Cr39), from the N-methylene proton, in order to implement the quality control detailed in Chapter 2.

Figure 12 presents an example of how prior knowledge looks using a 3D representation and a stack plot for Cr3.03ppm, GABA and NAA. In the last two, the cross peaks at an angle on 45 degrees produced by JPRESS can be easily observed. Note that the NAA peak at 4.2 is not part of the region of interest (ROI) considered, and as such is not presented in Figure 12(e).

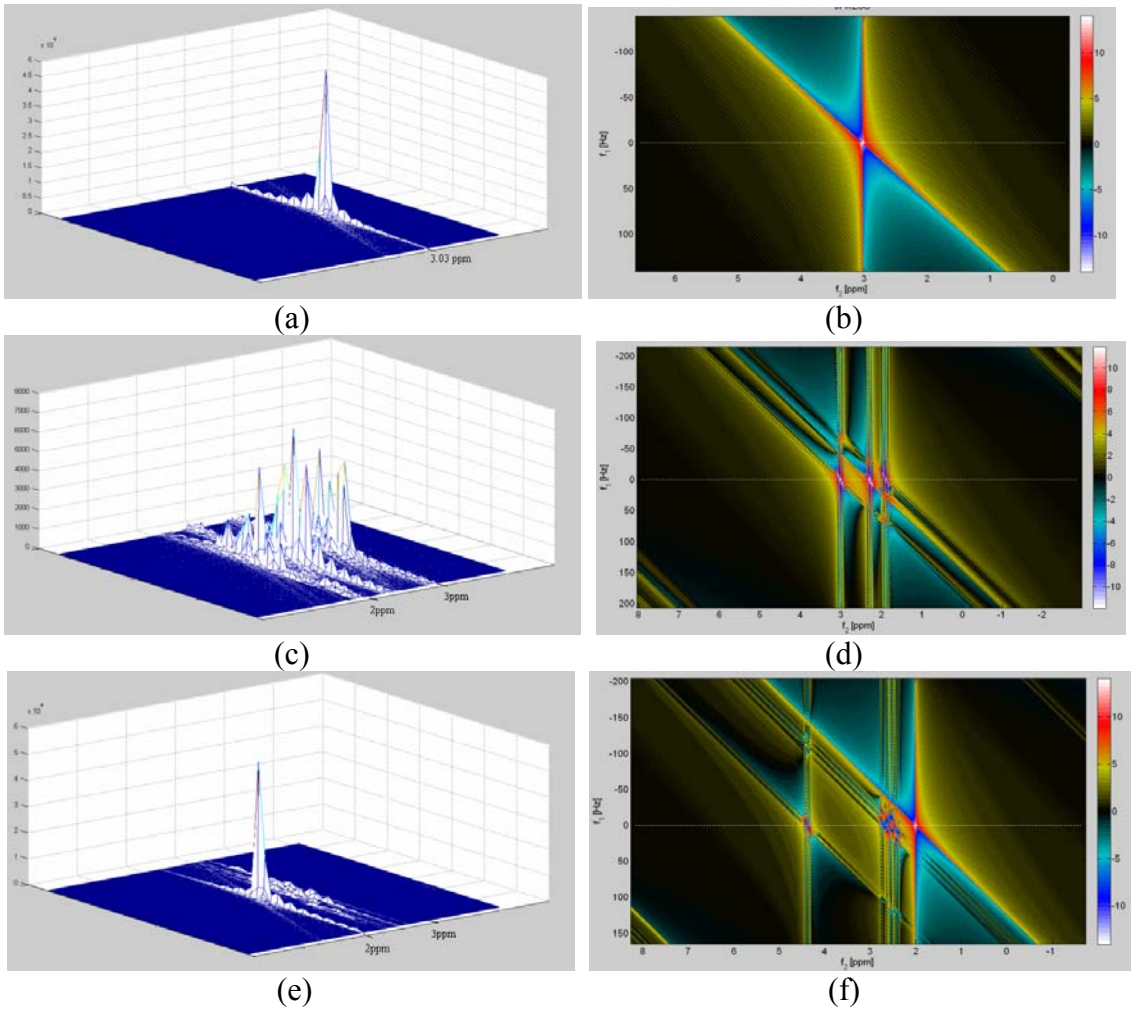

Figure 12. (a) Prior knowledge generated for Cr303 and (b) its stack representation; (c) prior knowledge generated for GABA and (d) its stack representation; (e) prior knowledge generated for NAA and (f) its stack representation.

Figure 13 presents the combination of all the prior knowledge generated for JPRESS at 2.89T, where the dispersion of the cross peaks can be appreciated. Only the region of interest (ROI) considered for the original spectra and the prior knowledge is presented in these figures. Prior knowledge generated for Siemens Avanto 1.5T followed the same process as in the previous case but with a value of T=1.5. The same group of metabolites was considered.

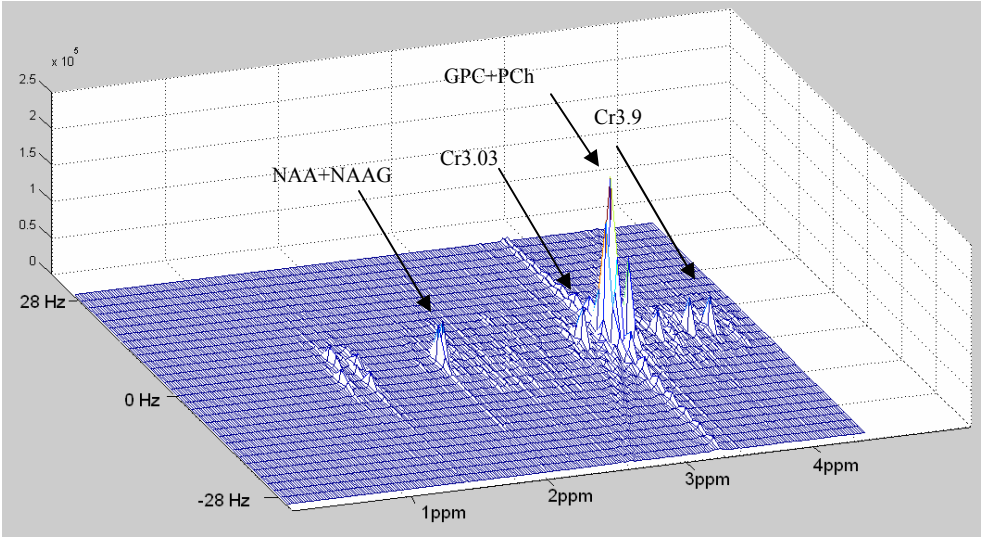

Figure 13. Combination of the total prior knowledge spectra generated for 3T JPRESS.

Calculation of Glx, t-cho and t-NAA

The modification of ProFit algorithm for obtaining also the concentrations of Glx, t-Cho and t-NAA was motivated by the fact that the literature typically reports those concentrations using 1D MRS, because the individual metabolites have a high level of overlapping. The process for obtaining these values is a post processing of the results obtained by ProFit and it does not imply a modification of the algorithm.

The concentration, C, is obtained by adding the individual concentrations of those metabolites before expressing the results as a ratio to creatine:

$$C(Glx) = C(G\ln) + C(Glu), \tag{18}$$

$$C(tCho) = C(Cho) + C(GPC) + C(PCh), \tag{19}$$

$$C(tNAA) = C(NAA) + C(NAAG). \tag{20}$$

Once the concentration values have been obtained the results can then be expressed also as a ratio to Creatine.

As for obtaining the CRLBs, they are calculated following the same concepts presented in the section 2.6 of Chapter 2. The CRLB is obtained as a percentage of the square root of the variance (*Var*) compared to the metabolite concentration. The variance (*Var*) of each combination of metabolites is obtained from the Fisher Matrix (*F*), by adding the corresponding values; for example the variance of Glx, is obtained by adding the variance of Glu, *F(Glu,Glu)* using Glu as an index to access the Fisher matrix, plus the variance of Gln, *F(Gln,Gln)*, plus the variance of Glu in Gln, plus the variance of Gln in Glu, which are the same, *2F(Glu,Gln)*. Formally:

$$\begin{aligned} CRLB(Glx) &= \frac{\sqrt{Var(Glx)}}{C(Glx)} \cdot 100 \\ Var(Glx) &= F(Glu,Glu) + F(G\ln,G\ln) + 2F(Glu,G\ln) \end{aligned} \quad , \qquad (21)$$

$$\begin{aligned} CRLB(tCho) &= \frac{\sqrt{Var(tCho)}}{C(tCho)} \cdot 100 \\ Var(tCho) &= F(GPC,GPC) + F(PCh,PCh) + F(Cho,Cho) + , \\ &+2F(GPC,PCh) + 2F(GPC,Cho) + 2F(PCh,Cho) \end{aligned} \qquad (22)$$

$$\begin{aligned} CRLB(tNAA) &= \frac{\sqrt{Var(tNAA)}}{C(tNAA)} \cdot 100 \\ Var(tNAA) &= F(NAA,NAA) + F(NAAG,NAAG) + 2F(NAA,NAAG) \end{aligned} \quad . \qquad (23)$$

3.2 Brain Metabolite Quantitation using Siemens 3T Trio and 1.5T Avanto MRI Scanners

One of the mechanisms for increasing metabolite specificity and for reducing CRLB is using scanners with higher magnetic fields (T). Siemens Trio and Siemens Avanto are two examples of scanners that work at 3T and 1.5T. This section will study the impact

that the increase in T produces in the specificity and quality of the measurements. The study will be made for both 1D PRESS and 2D JPRESS using both *in-vivo* and phantom data.

3.2.1 Methods and Materials

2D JPRESS and 1D PRESS sequences were implemented, as shown in Fig. 1, on a Siemens 3T Trio and a Siemens 1.5T Avanto scanners (Siemens Medical Systems, Germany) running on the VB15 platform. Ten healthy volunteers were scanned. For 2D MRS the parameters used were: *TR/TE=2.0s/30ms*, voxel size of *3x3x3 cm^3*, 8 averages per $\Delta t1$, 100 $\Delta t1$ increments and 2048 points in t_2. The parameters used for 1D PRESS were as follows: *TR/TE=2.0s/30ms*, voxel size of *2.5x2.5x2.5 cm^3* and 256 averages. Also, a white matter brain phantom containing fifteen metabolites (pH=7.3) was used for recording 20 *in-vitro* measurements both in 1D PRESS and 2D JPRESS. The metabolites included in the phantom and their concentration expressed as a ratio to creatine was: creatine (Cr) at 1, N-acetylaspartate (NAA) at 1.08, phosphorylcholine (PCh) at 0.085, free choline (Cho) at 0.12, aspartate (Asp) at 0.042, γ-aminobutyric acid (GABA) at 0.1, glucose (Glc) at 0.14, glutamine (Gln) at 0.22, glutamate (Glu) at 1.15, glutathione (GSH) at 0.28, lactate (Lac) at 0.057, myo-inositol (mI) at 0.5, N-acetylaspartylglutamate (NAAG) at 0.21, phosphoethanolamine (PE) at 0.47 and taurine (Tau) at 0.12.

1D PRESS spectra were processed using LC-Model in a Sun Sparc machine. 2D JPRESS spectra were quantified using a ProFit implementation in Matlab running on a 2.8GHz Intel processor with Windows XP. The prior knowledge used by ProFit when processing *in-vivo* spectra contained the 20 metabolites described in section 3.1. Two

extra prior knowledge sets were generated, one for 2.98T and another for 1.5T, that contained only the fifteen metabolites present in the phantom solution, in order to process efficiently the phantom spectra. The accuracy of the quantitation was characterized using Cramer-Rao lower bounds (CRLB) [7], where only values with CRLB<20% were considered valid. When using ProFit, the quantitation results from a spectrum were considered valid only if the ratio of Cr3.91 to Cr3.03 was smaller that 1.3.

The data collected provided information for: (1) comparing the metabolite concentrations provided by 1D PRESS spectra at 1.5T and 3T using LC-Model (both *in-vivo* and phantom) and (2) comparing the metabolite concentrations provided by 2D JPRESS spectra at 1.5T and 3T using ProFit (both *in-vivo* and phantom).

3.2.2 Results and Discussions using 1D MRS

Table I and Table II present the concentration values obtained using 1D PRESS with LC-Model at 1.5T and 3T for *in-vivo* (Table I) and phantom (Table II) respectively. The first column, % Valid, indicates the percentage of the total spectra that produced a valid result, with CRLB<20%, for that particular metabolite. The column Ratio/Cr indicates the average ratio to Creatine of the valid measurements, including the standard deviation, and the column CRLB indicates the average value of the CRLBs of the valid measurements, including the standard deviation.

As can be seen, some of the metabolites only indicate NBS (No Basis Set), meaning that LC-Model does not include prior knowledge for that metabolite. The algorithm used by LC-Model does not impose any limit in the number of metabolites that can be included as part of the prior knowledge, nevertheless the prior knowledge considered by

LC-Model does not consider Cho, Gly, GSH, PE and Asc. Although it may seem that the prior knowledge should contain as many metabolites as possible, the inclusion of too many metabolites will cause problems, especially if working in 1D, because the orthogonality of the basis set will increase. This increase in orthogonality will imply an increase in CRLB, which will in turn reduce the number of valid quantitations. This fact caused that the designers of LC-Model did not consider those metabolites as part of the prior knowledge. Nevertheless, these metabolites have been included in these tables as a way of facilitating comparison with the results obtained by 2D JPRESS with ProFit.

Table I. Concentrations of in-vivo metabolites using 1D PRESS and LC-Model at 1.5T and 3T.

	1.5 T 1D PRESS LC-Model *in-vivo*			**3 T 1D PRESS LC-Model *in-vivo***		
	% Valid	**Ratio/Cr**	**CRLB**	**% Valid**	**Ratio/Cr**	**CRLB**
Cr	100	1	2.9±0.4	100	1	1.2±0.4
NAA	100	1.2±0.14	3.9±0.99	100	1.36±0.18	1.3±0.67
GPC	100	0.23±0.02	4.9±1.2	100	0.14±0.03	3.09±4.3
PCh	0	-	-	0	-	-
Cho	NBS	NBS	NBS	NBS	NBS	NBS
Ala	0	-	-	0	-	-
Asp	60	0.24±0.03	18±1.09	100	0.55±0.09	9.7±2.6
GABA	0	-	-	50	0.35±0.14	15±2.12
Glc	0	-	-	20	0.22±0.09	12±2.8
Gln	10	0.43±0.00	14.0±0.00	40	0.23±0.21	16±2.7
Glu	100	0.71±0.12	13±2.06	100	1.3±0.2	4.7±0.8
Gly	NBS	NBS	NBS	NBS	NBS	NBS
GSH	NBS	NBS	NBS	NBS	NBS	NBS
Lac	0	-	-	0	-	-
mI	100	0.68±0.07	4.4±1.4	100	0.74±0.06	2.5±0.5
NAAG	10	0.17±0.00	17±0.00	30	0.15±0.08	10±2.1
PE	NBS	NBS	NBS	NBS	NBS	NBS
Tau	0	-	-	70	0.25±0.05	16.7±2.4
Scy	0	-	-	60	0.04±0.00	15±2.3
Asc	NBS	NBS	NBS	NBS	NBS	NBS
NAA+NAAG	100	1.26±0.09	3.3±0.67	100	1.45±0.14	1.2±0.42
GPC+PCh+Cho	100	0.23±0.02	4.9±1.2	100	0.14±0.02	2±0.66
Gln+Glu	100	0.96±0.12	13.1±2.8	100	1.41±0.27	4.9±0.87

Table II. Concentrations of phantom metabolites using 1D PRESS and LC-Model at 1.5T and 3T.

	Phantom Value	1.5 T 1D PRESS LC-Model Phantom			3 T 1D PRESS LC-Model Phantom		
		% Valid	**Ratio/Cr**	**CRLB**	**% Valid**	**Ratio/Cr**	**CRLB**
Cr	1	100	1	2.8±0.68	100	1	2.44±0.52
NAA	1.08	100	1.3±0.2	3.2±0.9	100	1.2±0.06	2.5±0.5
PCh	0.08	100	0.22±0.2	8.5±4.3	100	0.2±0.00	7.72±2.7
Cho	0.12	NBS	NBS	NBS	NBS	NBS	NBS
Asp	0.04	0	-	-	0	-	-
GABA	0.1	0	-	-	0	-	-
Glc	0.14	75	0.38±0.06	14.2±1.7	90	0.43±0.07	15.3±2.1
Gln	0.22	0	-	-	5	0.33±0.00	18±0.00
Glu	1.15	100	1.3±0.2	9.3±2.3	100	2.05±0.14	6.06±1.1
GSH	0.28	NBS	NBS	NBS	NBS	NBS	NBS
Lac	0.05	55	0.12±0.01	18.2±3.2	10	0.12±0.01	15.5±0.7
mI	0.5	100	0.76±0.08	6.62±1.7	100	0.93±0.04	5.5±12
NAAG	0.21	70	0.36±0.12	14.6±4.4	50	0.17±0.03	14.3±2.5
PE	0.47	NBS	NBS	NBS	NBS	NBS	NBS
Tau	0.12	0	-	-	0	-	-
NAA+NAAG	1.29	100	1.59±0.19	2.72±0.57	100	1.36±0.07	2.1±0.3
PCh+Cho	0.2	100	0.23±0.01	5.5±1.3	100	0.27±0.01	3.38±0.6
Gln+Glu	1.37	100	1.37±0.2	9.58±2.1	100	2.14±0.17	6.06±1.06

As can be observed, just moving from 1.5T to 3T in 1D PRESS increases the number of detectable metabolites, defining detectable metabolites as the ones that at least are detected 40% of the times (at least a value of 40 in the % Valid column). In *in-vivo* it goes from 6 out of 20 in 1.5T to 10 out of 20 in 3T. LC-Model does not detect, both at 3T and 1.5T, Cho, Gly, GSH, PE and Asc because they are not included as part of the prior knowledge. Also, PCh, Ala, GABA, Glc, Gln, Lac, NAAG, Tau and Scy are not detected at 1.5T although they are part of the prior knowledge, while at 3T only PCh, Ala, Glc, Lac and NAAG are not detectable. This means that by moving from 1.5T to 3T in 1D spectroscopy GABA, Gln, Lac, Tau and Scy are now detectable.

The improvement in the delectability of the metabolites is reflected in the reduction in the average CRLB caused by moving from 1.5T to 3T. In *in-vivo* measurements there is a

reduction of the average CRLB in all detectable metabolites while the same is also true for phantom measurements. Figure 14 shows the reduction in CRLB in the commonly detectable *in-vivo* metabolites at 3T and 1.5T using 1D spectroscopy. The average CRLB is reduced for all detectable metabolites, and also, in the cases of Cr, NAA, GPC, Asp, Glu, mI, t-NAA, Glx and t-cho, that difference is statistically meaningful with $p<0.05$, i.e. there is a statistically meaningful improvement in metabolite specificity in 1D spectroscopy caused by moving from 1.5T to 3T.

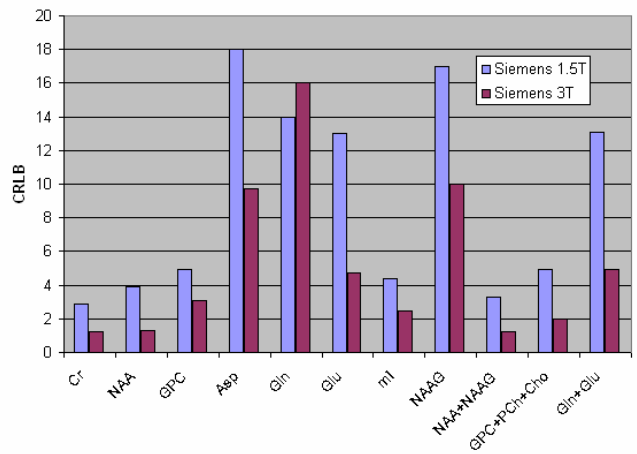

Figure 14. Comparison of CRLBs between 1.5T and 3T of the detectable metabolites using 1D PRESS and LC-Model.

3.2.3 Results and Discussions using 2D MRS

Table III and Table IV present the metabolite concentration for *in-vivo* and phantom measurements respectively, using 2D JPRESS with ProFit. None of the data considered, both *in-vivo* and phantom, had to be eliminated because Cre3.9>1.3.

The values confirm the conclusions obtained in 1D spectroscopy: by going from 1.5T to 3T the number of metabolites increases and the CRLB is reduced. In this case, 1.5T ProFit is able to detect (at a 40% level) 15 out of the 20 metabolites (only PCh, Cho, Asp,

Gly and Tau are not detectable), while 3T detects all metabolites except PCh. It is noticeable that at 1.5T Cho, Gly and Tau are never quantitated correctly, which is probably because they are heavily overlapped with other metabolites. CRLB are reduced for all metabolites at 3T except for Lac and Ala, while PCh remains constant.

Similar results are reproduced in the concentrations values obtained for the phantom data. In this case, at 1.5T only PE and Asc are not detectable, while at 3T all metabolites are detectable. CRLBs are reduced for all metabolites except for Lac and Tau CRLBs which remain constant.

Table III. Concentrations of in-vivo metabolites using 2D JPRESS and ProFit at 1.5T and 3T.

	1.5 T 2D JPRESS ProFit *in-vivo*			**3 T 2D JPRESS ProFit *in-vivo***		
	% Valid	**Ratio/Cr**	**CRLB**	**% Valid**	**Ratio/Cr**	**CRLB**
Cr303	100	1±0	1.32±0.1	100	1±0	0.82±0.13
Cr391	100	0.81±0.12	2.88±1.1	100	0.9±0.04	1.61±0.26
NAA	100	1.21±0.23	1.74±0.8	100	1.5±0.2	0.76±0.23
GPC	90	0.18±0.07	9.93±4.8	90	0.16±0.03	8.4±2.8
PCh	40	0.11±0.05	11.5±7.3	20	0.13±0.04	11.5±4.9
Cho	0	-	-	40	0.04±0.00	14.2±2.8
Ala	90	0.41±0.19	5.33±2.9	50	0.08±0.01	12.6±1.67
Asp	30	0.23±0.02	13.3±2.5	100	0.55±0.1	5.8±0.41
GABA	80	0.27±0.1	13.2±4.6	100	0.35±0.06	5.3±0.65
Glc	100	0.71±0.21	6.65±2.5	100	0.65±0.1	4.6±0.91
Gln	90	0.35±0.08	15.6±5.7	100	0.43±0.06	6.1±1.32
Glu	100	1.28±0.09	4.8±2.3	100	1.26±0.11	2.4±0.46
Gly	0	-	-	90	0.15±0.2	13.1±3.05
GSH	100	0.17±0.04	9.9±4.4	100	0.24±0.06	4.1±0.91
Lac	100	0.17±0.05	9.2±3.2	90	0.12±0.03	9.4±2.37
mI	100	1.02±0.13	3.8±1.5	100	1.01±0.07	2.3±0.38
NAAG	100	0.28±0.15	8.8±5.6	80	0.31±0.03	4.6±2.08
PE	90	0.4±0.15	11.9±6	100	0.52±0.1	5.2±0.78
Tau	0	-	-	80	0.12±0.01	16.5±0.7
Scy	70	0.03±0.01	13.8±5	100	0.04±0.01	10.5±3.47
Asc	60	0.35±0.15	10.2±6.3	100	0.59±0.1	3.5±0.59
NAA+NAAG	100	1.49±0.14	0.74±0.3	100	1.8±0.15	0.43±0.05
GPC+PCh+Cho	100	0.24±0.04	1.81±0.9	100	0.29±0.02	1.61±0.38
Gln+Glu	100	1.63±0.09	3.52±1.5	100	1.7±0.13	2.12±0.33

Table IV. Concentrations of phantom metabolites using 2D JPRESS and ProFit at 1.5T and 3T.

	Phantom Value	1.5 T 2D JPRESS ProFit Phantom			3 T 2D JPRESS ProFit Phantom		
		% Valid	Ratio/Cr	CRLB	% Valid	Ratio/Cr	CRLB
Cr303	1	100	1	0.56±0.31	100	1±0	0.43±0.03
Cr391	1	100	0.93±0.07	0.94±0.49	100	1±0.04	0.66±0.06
NAA	1.08	100	1.11±0.07	0.65±0.52	100	1.13±0.05	0.45±0.09
PCh	0.08	100	0.11±0.01	2.48±1.91	100	0.12±0.01	1.82±0.31
Cho	0.12	100	0.1±0.01	2.64±2.32	100	0.1±0.01	2.03±0.64
Asp	0.04	0	-	-	70	0.14±0.03	12±3.5
GABA	0.1	100	0.24±0.06	7.5±3.99	100	0.26±0.08	4.39±2.63
Glc	0.14	100	0.34±0.04	6.2±3.82	95	0.28±0.08	6.4±2.6
Gln	0.22	90	0.19±0.05	11.8±3.65	90	0.2±0.04	6.6±1.3
Glu	1.15	100	1.17±0.07	2.31±1.37	100	1.24±0.06	1.31±0.16
GSH	0.28	100	0.07±0.02	10.7±4.48	100	0.26±0.02	2.07±0.21
Lac	0.05	100	0.08±0.01	9.4±4.2	90	0.06±0.01	9.6±2.3
mI	0.5	100	0.8±0.03	1.91±1.11	100	1.05±0.07	1.21±0.16
NAAG	0.21	90	0.17±0.05	4.6±2.5	75	0.15±0.03	2.8±0.43
PE	0.47	5	0.22±0	9±0	95	0.24±0.06	6.1±2.7
Tau	0.12	80	0.1±0.04	11.5±3.4	40	0.11±0.04	12±3.33
NAA+NAAG	1.29	100	1.26±0.03	0.43±0.21	100	1.17±0.07	0.37±0.04
PCh+Cho	0.2	100	0.22±0.01	0.84±0.43	100	0.23±0.01	0.64±0.05
Gln+Glu	1.37	100	1.36±0.12	2.08±1.18	100	1.43±0.08	1.39±0.18

Figure 15 shows the reduction in CRLB in the commonly detected *in-vivo* metabolites at 3T and 1.5T using 2D spectroscopy. Also, the reduction in the average CRLB is statistically meaningful at a level of $p<0.01$ for Cr, NAA, Asp, GABA, Gln, Glu, GSH, mI, NAAG, Asc and PE, i.e. there is a statistically meaningful improvement in the specificity of the metabolites in 2D spectroscopy caused by the increase of the magnetic field from 1.5T to 3T.

In general, the results reported for *in-vivo* concentration of metabolites at 3T are in accordance with the values reported in the literature [27]. There are some exceptions: Gln, is reported in the literature with a concentration of 0.21 while in our case the concentration in 0.35 at 1.5T and 0.43 at 3T; Glc is reported with a concentration of 0.36, while our results indicate a concentrations of 0.71 at 1.5T and 0.65 at 3T, and GABA is

reported with a concentration of 0.17, and in our case the concentration is 0.27 at 1.5T and 0.35 at 3T.

As for the phantom results, focusing on 2D MRS at 3T, although the best part of them are within the correct range, there are few metabolites for which the concentration reported are very different from the expected one, mainly: PE has a relative concentration of 0.47 and the reported concentration is 0.24, mI has a concentration of 0.5 while the reported concentration is 1.05, Glc has a concentration of 0.4 and the reported concentration is 0.28, and GABA has a concentration of 0.1 and the reported concentration is 0.26. These differences are caused by: (1) quality of the signal and (2) biases of ProFit. Regarding the quality of the signal, CRLB measures the quality of the fit not the quality of the signal, the quality of the signal is determined by Cre3.9<1.3. This implies that MR signals with water suppression problems have been considered valid, which may affect the quantitation of some metabolites. Regarding the biases of ProFit, its authors highlight a tendency of Glc, Asp and PE, for being overestimated and tendency for Gln of being underestimated [27], results that are to a large extent confirmed by the values presented here.

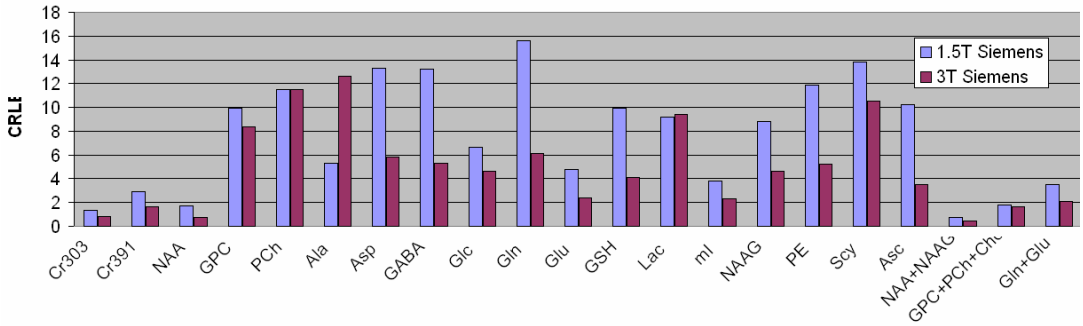

Figure 15. Comparison of CRLBs at 1.5T and 3T of the detectable metabolites using 2D JPRESS and ProFit.

3.2.4 Conclusions

The results of this study indicate that an increase of the magnetic field implies an increment in the number of metabolites detected and a reduction in the CRLBs, being this reduction statistically meaningful for a relevant group of metabolites. Also these facts seem to be independent of the dimensionality of the spectral sequence used (1D or 2D).

3.3 Metabolite Quantitation: 2D JPRESS versus 1D PRESS

In theory, the increase in dimensionality should cause an increase in the specificity of metabolite concentrations due to the fact that metabolites are easily resolved in the second dimension. The goal of this section is to check if that assumption is true and to which extent going from 1D to 2D reduces CRLBs of metabolites.

The data obtained in the previous section can be used for this study as it allows to (1) compare the metabolite concentrations at 1.5T provided by 1D spectroscopy (PRESS quantitated using LC-Model) with the ones provided by 2D spectroscopy (JPRESS quantitated with ProFit) and (2) compare metabolite concentrations at 3T provided by 1D spectroscopy with the ones provided by 2D spectroscopy. When comparing spectral data with different dimensions, it has also to be considered that the algorithms used for 1D quantitation and 2D quantitation are different algorithms, so the may play a role in the different quality of the quantitation. For the purpose of this study it will be considered that the algorithms do not play a role in the quality of the quantitation, which it is assumed will be only affected by prior knowledge and the quality of the input data. This assumption, in itself, is acceptable because LC-Model and ProFit are actually fairly

similar algorithms as they are both based in the fitting of prior knowledge to the input data using a non-linear optimization process. Methods and Materials are not described as they are exactly the ones presented in the previous section.

3.3.1 Results and Discussion

Table V presents again the concentrations and CRLBs at 3T obtained using 1D PRESS and 2D JPRESS for *in-vivo* (the data has been put together here for comparison purposes).

Table V. Concentrations of cerebral metabolites *in-vivo* at 3T with (left) 1D PRESS-LC-Model and (right) 2D JPRESS and ProFit .

	3T 1D PRESS LC-Model *in-vivo*			**3 T 2D JPRESS ProFit *in-vivo***		
	% Valid	**Ratio/Cr**	**CRLB**	**% Valid**	**Ratio/Cr**	**CRLB**
Cr303	100	1	1.2±0.4	100	1±0	0.82±0.13
Cr391	NBS	NBS	NBS	100	0.9±0.04	1.61±0.26
NAA	100	1.36±0.18	1.3±0.67	100	1.5±0.2	0.76±0.23
GPC	100	0.14±0.03	3.09±4.3	90	0.16±0.03	8.4±2.8
PCh	0	-	-	20	0.13±0.04	11.5±4.9
Cho	NBS	NBS	NBS	40	0.04±0.00	14.2±2.8
Ala	0	-	-	50	0.08±0.01	12.6±1.67
Asp	100	0.55±0.09	9.7±2.6	100	0.55±0.1	5.8±0.41
GABA	50	0.35±0.14	15±2.12	100	0.35±0.06	5.3±0.65
Glc	20	0.22±0.09	12±2.8	100	0.65±0.1	4.6±0.91
Gln	40	0.23±0.21	16±2.7	100	0.43±0.06	6.1±1.32
Glu	100	1.3±0.2	4.7±0.8	100	1.26±0.11	2.4±0.46
Gly	NBS	NBS	NBS	90	0.15±0.2	13.1±3.05
GSH	NBS	NBS	NBS	100	0.24±0.06	4.1±0.91
Lac	0	-	-	90	0.12±0.03	9.4±2.37
mI	100	0.74±0.06	2.5±0.5	100	1.01±0.07	2.3±0.38
NAAG	30	0.15±0.08	10±2.1	80	0.31±0.03	4.6±2.08
PE	NBS	NBS	NBS	100	0.52±0.1	5.2±0.78
Tau	70	0.25±0.05	16.7±2.4	80	0.12±0.01	16.5±0.7
Scy	60	0.04±0.00	15±2.3	100	0.04±0.01	10.5±3.47
Asc	NBS	NBS	NBS	100	0.59±0.1	3.5±0.59
NAA+NAAG	100	1.45±0.14	1.2±0.42	100	1.8±0.15	0.43±0.05
GPC+PCh+Cho	100	0.14±0.02	2±0.66	100	0.29±0.02	1.61±0.38
Gln+Glu	100	1.41±0.27	4.9±0.87	100	1.7±0.13	2.12±0.33

Going from 1D to 2D spectroscopy produces an increase in the number of metabolites that are quantified, from 10 out of 20 in 1D to 19 out of 20 in 2D. The only metabolite that is not detectable (at a level of 40%) in 2D JPRESS is PCh. That is expected because of the heavy overlap between GPC, PCh and Cho. Using 1D spectroscopy, Cho, Gly, GSH, PE and Asc are not detectable because they are not part of the prior knowledge, while PCh, Ala, Glc, Lac and NAAG are not detectable because 1D does not resolve them properly.

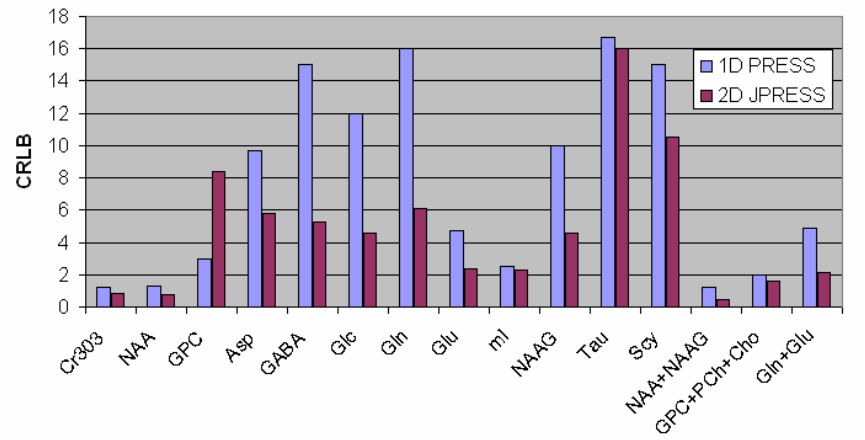

Figure 16. Comparison of CRLBs at 3T of the detectable metabolites using 1D PRESS and 2D JPRESS.

Figure 16 presents the changes in CRLBs of the metabolites that are detected both in 1D and in 2D. As can be seen there is a reduction in all the metabolites in 2D (with the exception of GPC). In the cases of Asp, GABA, Glc, Gln, Glu, NAAG, Scy, t-Cho, t-NAA and Glx, this reduction is statistically meaningful at a level of $p<1\%$.

At 1.5T the results are similar to the ones presented for 3T (the values were presented in Tables I and III). Using the *in-vivo* results, 1D PRESS is able to identify 6 out of the 20 metabolites, while 2D JPRESS detects 16 out of the 20. Comparing with the previous

results at 3T, the effect of the magnetic field for metabolite specificity is highlighted again. For 1D PRESS, considering the metabolites that have prior knowledge, PCh, Ala, GABA, Glc, Lac, Tau, NAAG and Scy are not detectable, while in 2D JPRESS only Cho, Asp, Gly and Tau are not detectable.

Figure 17 compares the CRLBs of the detectable metabolites at 1.5T for 1D PRESS and 2D JPRESS. As in the 3T case a general reduction in the average CRLB is observed for all metabolites, except for GPC (that increases in 2D) and Gln that basically remains constant.

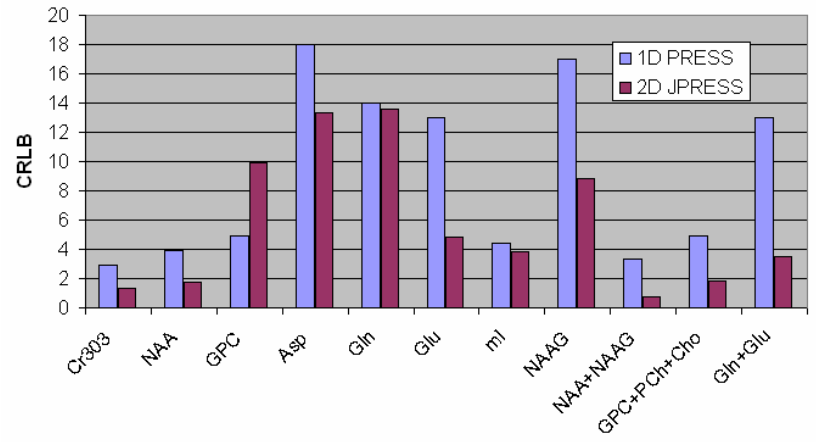

Figure 17. Comparison of CRLBs at 3T of the detectable metabolites using 1D PRESS and 2D JPRESS.

Similar comparisons can be done for the phantom data using the values presented in Table I thought Table IV, and the results are in agreement with the ones reported for *in-vivo*.

3.3.2 Conclusions

The results of this study indicate that an increase in the dimensionality of the spectral data increases the specificity of the metabolites, which implies that a higher number of metabolites are detected and that there is a reduction of the CRLBs, being this reduction

statistically meaningful for a relevant group of metabolites. These results seem to be independent from the magnetic field used.

These results confirm the hypothesis that 2D MRS is superior to 1D MRS because metabolites are easily resolved due to the extra dimensionality. Although 2D MR spectroscopy does not have the same importance as 1D MRS, results as the ones presented in this study should encourage the transition to multidimensional spectroscopy, specially if the quantitations want to be applied to the clinical environment, where the quality of the measurement is a must.

CHAPTER 4

QUANTITATION OF 2D COSY MR SPECTROSCOPY

Compared to JPRESS, COSY spectroscopy further improves spectral dispersion along the second dimension. In theory, this improved dispersion should facilitate a better resolution of different metabolites, which in turn should produce an increase in metabolite's specificity and a reduction in the CRLBs values.

4.1 Modifications of ProFit for COSY 3T Siemens Trio

ProFit algorithm was developed for quantitation of 2D JPRESS signals. Although the fitting algorithm is independent of the sequence implemented, it affects a series of parameters of the code, including prior knowledge. The elements that have been changed are: (1) reversal of the spectrum, (2) generation of prior knowledge for COSY 3T using GAMMA, (3) calculation of total concentrations and CRLBs values for Glx, t-cho and t-NAA, (4) filter modification for reconstruction, and (5) modification of the area considered for fitting. The first and third elements have already been described in the previous chapter.

Generation of Prior Knowledge for COSY

GAMMA code for the simulation of COSY spectra was generated using C++. The code was fairly similar to the one used for JPRESS generation. The main modifications were the change of the spectral window considered and the change of the third rf pulse from a flip angle of 180 degrees to 90 degrees. Prior knowledge for the same 20 metabolites detailed in the previous chapter was generated using the following parameters:

TR/TE=2s/30ms, B_0=*2.89 T*, 100 $\Delta t1$ increments and 2048 points in t_2. Figure 18 presents the combination of the 20 metabolites considered for prior knowledge. It can be observed that the spectral dispersion is improved when compared to JPRESS in Figure 13.

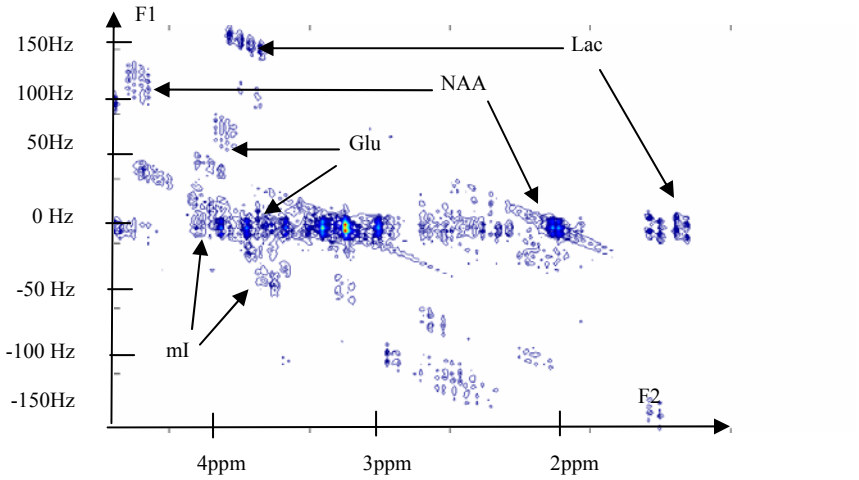

Fig. 18 Combination of 20 COSY spectra generated for prior knowledge.

Filter Modifications for Reconstruction

The information contained by COSY data does not show the cross peaks without using the proper filters. COSY turns out to be very sensitive to the types of filters used and the values of those filters. If the correct filters are not used, cross peaks will not appear. Filters are applied during data reconstruction in both t_1 and t_2 and should also be applied when the prior knowledge is being constructed. A squared sine bell filter is applied to t_1 and a skewed sine bell filter with a skew factor of 0.5 is applied to t_2 [11]. Assuming 100 increments in t_1 and 2048 points in t_2 the filters are defined as:

$$F(t_1) = \left(\sin\left(\frac{\pi t_1}{100} \right) \right)^2, \qquad (18)$$

$$F(t_2) = \sin\left(\pi\left(\frac{t_2 - 1}{2048}\right)^{skew}\right), \qquad (19)$$

Modification of the Fitting Area

One of the main differences between JPRESS and COSY is the improved spectral dispersion of COSY. ProFit has been designed to process JPRESS data, which implies that the window used for the minimization process is designed to capture the data according to the spectral dispersion provided by JPRESS. The original region of interest (ROI) considered by Profit is $1.3\ ppm < f_2 < 4.1ppm$ and $-28\ Hz < f_1 < 28Hz$. This window is not big enough to capture all the cross peaks provided by COSY, so a bigger window has been implemented, ranging from 1ppm to 4.5 ppm in f_2 and from -170 Hz to 170 Hz in f_1. Figure 19 presents a typical COSY spectrum with the original ProFit window considered for the minimization process (in red) and the extended window that has been implemented to capture all the extra data provided by COSY.

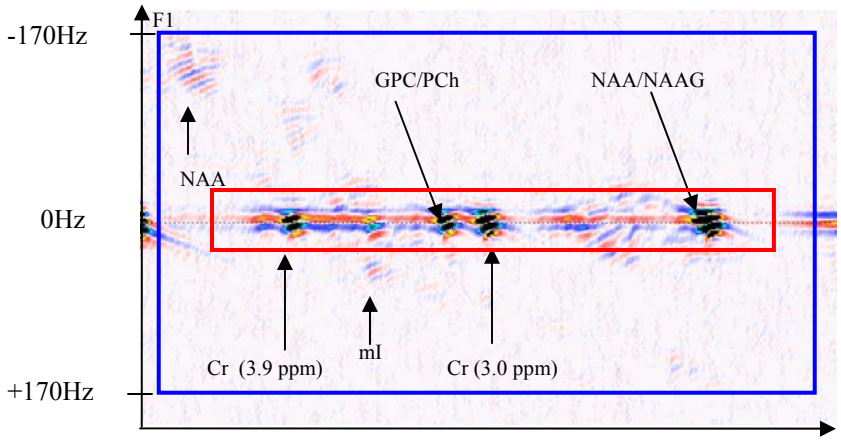

Figure 19. Original ProFit ROI considered for fitting (red) and extended ROI considered for COSY (blue).

The area needed to be processed for the minimization process is eight time bigger for COSY that for JPRESS which implies a relevant increment in the processing time needed to obtain concentrations.

4.2 2D COSY vs. 2D JPRESS Quantitation of Metabolites at 3T

The extra dispersion that COSY data shows when compared with JPRESS has benefits, the main one being that the extra dispersion reduces the orthogonality of the prior knowledge which, in turn should reduce the CRLBs of the quantitations. This section tests if this assumption is valid by comparing *in-vivo* and phantom COSY concentration results with the JPRESS values obtained in Chapter 3.

4.2.1 Methods and Materials

A maximum-echo sampling 2D L-COSY sequence containing three slice-selective RF pulses (90^0, 180^0, 90^0) was implemented on a Siemens 3T Trio-Tim scanner (Siemens Medical Systems, Germany), as presented in Figure 2. The following parameters were used: *TR/TE=2s/30ms*, $3x3x3cm^3$ voxel, 8 averages per Δt_1 and 100 Δt_1 increments. A white matter brain phantom containing fifteen metabolites (pH=7.3) was used for processing 10 *in vitro* measurements. Eight healthy volunteers were investigated with the 2D MRS voxel localized in the occipital white/gray matter area.

COSY spectra were quantified using a modified ProFit on a 2.8GHz Intel processor with Windows XP. The prior knowledge used by ProFit when processing *in-vivo* spectra contained the 20 metabolites described in section 3.1. An extra prior knowledge set was generated that contained only the fifteen metabolites present in the phantom solution. The

accuracy of the quantitation was characterized using Cramer-Rao lower bounds (CRLB) [6,7], only values with CRLB<20% were considered valid. Only spectrum for which Cre3.9<1.3 were accepted.

4.2.2 Results and Discussion

Table VI presents the concentrations results obtained using in-vivo COSY data. Again, the first column, % Valid, indicates the percentage of the total spectra that produced a valid result (CRLB<20%), the column Ratio/Cr indicates the average ratio to Creatine of the valid measurements, including the standard deviation, and the column CRLB indicates the average value of the CRLB including the standard deviation.

Table VI. Concentrations of in-vivo metabolites using at 3T with (left) 2D COSY and (right) 2D JPRESS.

	3 T 2D COSY ProFit *in-vivo*			**3 T 2D JPRESS ProFit *in-vivo***		
	% Valid	**Ratio/Cr**	**CRLB**	**% Valid**	**Ratio/Cr**	**CRLB**
Cr303	100	1±0	0.48±0.26	100	1±0	0.82±0.13
Cr391	100	0.87±0.15	0.97±0.59	100	0.9±0.04	1.61±0.26
NAA	100	1.4±0.32	0.56±0.27	100	1.5±0.2	0.76±0.23
GPC	90	0.11±0.05	4.8±4.8	90	0.16±0.03	8.4±2.8
PCh	90	0.11±0.05	4±4.42	20	0.13±0.04	11.5±4.9
Cho	90	0.1±0.01	2.37±0.77	40	0.04±0.00	14.2±2.8
Ala	60	0.11±0.03	5.2±3.03	50	0.08±0.01	12.6±1.67
Asp	90	0.4±0.1	4.7±3.4	100	0.55±0.1	5.8±0.41
GABA	60	0.34±0.27	7.6±4	100	0.35±0.06	5.3±0.65
Glc	70	0.28±0.11	4.2±2.9	100	0.65±0.1	4.6±0.91
Gln	40	0.25±0.16	10±7.1	100	0.43±0.06	6.1±1.32
Glu	100	1.37±0.35	2.28±1.77	100	1.26±0.11	2.4±0.46
Gly	70	0.12±0.08	7.38±4	90	0.15±0.2	13.1±3.05
GSH	90	0.16±0.08	4.02±2.9	100	0.24±0.06	4.1±0.91
Lac	60	0.17±0.08	4.6±2.06	90	0.12±0.03	9.4±2.37
mI	100	0.86±0.1	2.02±1.28	100	1.01±0.07	2.3±0.38
NAAG	70	0.35±0.1	1.71±1.22	80	0.31±0.03	4.6±2.08
PE	80	0.21±0.11	5±0.28	100	0.52±0.1	5.2±0.78
Tau	90	0.2±0.07	4.07±1.31	80	0.12±0.01	16.5±0.7
Scy	90	0.05±0.00	4.6±2.7	100	0.04±0.01	10.5±3.47
Asc	80	0.28±0.18	3.48±1.2	100	0.59±0.1	3.5±0.59
NAA+NAAG	100	1.6±0.23	0.27±0.04	100	1.8±0.15	0.43±0.05
GPC+PCh+Cho	100	0.29±0.04	0.86±0.46	100	0.29±0.02	1.61±0.38
Gln+Glu	100	1.53±0.34	1.79±0.34	100	1.7±0.13	2.12±0.33

One *in-vivo* and one phantom spectra were eliminated because Cre3.9>1.3. The column on the right (3T 2D JPRESS ProFit *in-vivo*) presents the JPRESS results that were presented in Chapter 3, and are reproduced here for comparison purposes.

COSY is able to correctly quantify the 20 metabolites considered in the prior knowledge. The only metabolite that was not detected using JPRESS was PCh, that COSY is able to detect correctly. This result was expected because the extra dispersion provided by COSY helps to differentiate metabolites that are heavily overlapped such as GPC, PCh and Cho.

Figure 20 compares the CRLB values of COSY with the CRLBs of JPRESS for the 20 metabolites considered *in vivo*. It can be observed that there is a reduction in the CRLB in all metabolites, except for Gln and GABA that have a higher CRLB in COSY that in JPRESS. The reduction is especially noticeable in the GPC, PCh and Cho set of metabolites. Not only that, but for Cr303, Cr309, NAA, PCh, Cho, GPC, Ala, Asp, Gly, Lac, NAAG, Tau, Scy, t-NAA and t-Cho the different CRLBs are statistically meaningful with p<1%.

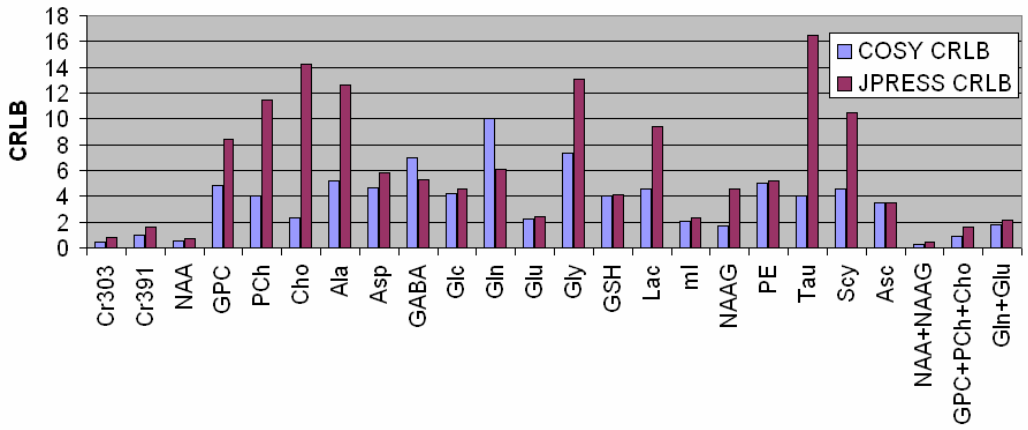

Figure 20. Comparison of COSY (in blue) and JPRESS (in red) CRLB at 3T for each metabolite of the prior knowledge.

The relative concentration values reported by COSY and JPRESS are similar with some exceptions. Some of the metabolites for which the concentration reported by JPRESS did not match the concentration reported in the literature, have been corrected by COSY, for example Gln, that is reported in the literature as a concentration of 0.21, JPRESS gave a concentration of 0.43 while COSY a concentration of 0.25; Glc for which the literature gives a concentration of 0.36, JPRESS gives a concentration of 0.65 while COSY gives a value of 0.28. Other cases like Asc the value reported by JPRESS is more similar to the concentration reported in the literature than the value reported by COSY.

Table VII presents the phantom results. As in the *in-vivo* case, there is a reduction in the CRLBs in almost all cases. Incidentally COSY was not able to detect Gln in the phantom measurements.

Table VII. Concentrations of phantom metabolites at 3T with (left) 2D COSY and (right) 2D JPRESS.

	Phantom Values	3 T 2D COSY ProFit Phantom			3 T 2D JPRESS ProFit Phantom		
		% Valid	Ratio/Cr	CRLB	% Valid	Ratio/Cr	CRLB
Cr303	1	100	1±0	0.3±0.03	100	1±0	0.43±0.03
Cr391	1	100	0.83±0.06	0.45±0.04	100	1±0.04	0.66±0.06
NAA	1.08	100	1.04±0.07	0.26±0.03	100	1.13±0.05	0.45±0.09
PCh	0.08	100	0.11±0.03	0.69±0.08	100	0.12±0.01	1.82±0.31
Cho	0.12	100	0.15±0.01	0.93±0.08	100	0.1±0.01	2.03±0.64
Asp	0.04	100	0.2±0.05	5.13±1.1	70	0.14±0.03	12±3.5
GABA	0.1	80	0.05±0	3.3±0	100	0.26±0.08	4.39±2.63
Glc	0.14	100	0.33±0.07	3.47±0.65	95	0.28±0.08	6.4±2.6
Gln	0.22	0	-	-	90	0.2±0.04	6.6±1.3
Glu	1.15	100	1.21±0.37	1.34±0.27	100	1.24±0.06	1.31±0.16
GSH	0.28	100	0.28±0.04	2.01±0.53	100	0.26±0.02	2.07±0.21
Lac	0.05	80	0.06±0.03	1.3±0.3	90	0.06±0.01	9.6±2.3
mI	0.5	100	1.02±0.06	0.72±0.1	100	1.05±0.07	1.21±0.16
NAAG	0.21	50	0.29±0.09	3.7±2.1	75	0.15±0.03	2.8±0.43
PE	0.47	100	0.22±0.09	4.89±1.72	95	0.24±0.06	6.1±2.7
Tau	0.12	100	0.24±0.05	2.95±0.44	40	0.11±0.04	12±3.33
NAA+NAAG	1.29	100	1.32±0.11	0.33±0.04	100	1.17±0.07	0.37±0.04
PCh+Cho	0.2	100	0.26±0.03	0.51±0.04	100	0.23±0.01	0.64±0.05
Gln+Glu	1.37	100	1.22±0.35	1.68±0.44	100	1.43±0.08	1.39±0.18

4.2.3 Conclusion

The results of this study indicate that the improved spectral dispersion provided by COSY increases metabolite specificity to the extent, that: (1) the 20 metabolites considered in the prior knowledge are quantitated and (2) COSY CRLBs are smaller that JPRESS CRLBs, to the extent that all CRLBs values obtained with COSY are smaller that 5% (except GABA and Gly that are 7%).

These results again justify the use of 2D spectroscopy over 1D, and, within 2D spectroscopy, highlight the benefits of using COSY over JPRESS.

CHAPTER 5

A PILOT STUDY ON THE MR SPECTROSCOPIC CHARACTERIZATION OF CEREBRAL METABOLITES IN LATE LIFE DEPRESSION PATIENTS USING 3T JPRESS

The previous chapters have focused on the technicalities of MR spectroscopic quantitation of metabolites. This chapter presents an example of a pilot study where MRS quantitation has been used to study and characterize patients diagnosed with late life depression. The goal of this chapter is present an example of how quantitation of metabolites can be used for a clinical patient cohort.

5.1 Introduction

Late life depression is a common mental disorder of elderly population. In general aging is associated with physiological changes in the brain, mainly the reduction of brain volume, and metabolic changes in certain metabolites. These metabolite changes provide the backdrop for behavioral disorders in the elderly, such as Alzheimer's disease or late-life depression [3].

There have already been studies related to late life depression using 2D and 1D MR spectroscopy. In 1D, these studies report an increase of the ratios of Cho and mI [17] in depressed patients, with quantitation being done using LC-Model. The limitations of using 1D for quantitation have already been discussed; in this case, it is especially relevant that one of the metabolites for which a variation is obtained, Cho, appears in an

area where metabolites are heavily overlapping. Similar studies have been done in 2D spectroscopy using COSY. The results in this case highlighted an increase in mI, PE and Glx for depressed patients, although the differences were not statistically meaningful. In this case quantitation was done manually by calculating the volume under specific regions selected by the operator.

The goal of this study is to characterize late life depression patients using 2D JPRESS spectroscopy and automated quantitation of metabolites using ProFit. This approach solves the limitations of previous approaches: (1) by using 2D spectroscopy, the problem of overcrowded spectra and overlap metabolites is partially solved and (2) by using automatic quantitation the dependence from the operator is solved.

5.2 Methods and Materials

2D JPRESS was implemented in a Siemens 3T Trio scanner (Siemens Medical Systems, Germany). The following parameters were used for 9 elderly healthy volunteers (mean age=70 years, std=5.24 years, range [62-76]) and 12 late life depression patients (mean age=69.3 years, std=6.31 years, range [60-79]): *TR/TE=2.5s/30ms*, *2.5x2.5x2.5* cm3 voxel, 4 averages per $\Delta t1$, *100* Δt_1 increments and 2048 points in t_2. 2D MRS voxels were localized in the frontal gray matter region. 2D JPRESS spectra were quantified using the modified ProFit version presented in Chapter 3 running on a 2.8GHz Intel processor with Windows XP. Prior knowledge included 20 metabolites simulated with GAMMA.

Up to now, ProFit has not been tested in clinical applications. In theory the value of Cr3.9 should be 1, expressing a ratio of 1 between Cr3.9 and Cr3.0. ProFit recommends to consider valid any data for which Cr3.9<1.3. Nevertheless, such assumption is too flexible for studies involving clinical applications and identification of markers of pathologies. In the case of this study, accepting as valid any spectra for which Cr3.9<1.3, implies that data with small values of Cr3.9 caused by water suppression will be considered for the study. Nevertheless, if it is known that the value of Cr3.9 has been affected, other metabolites would also have been affected, among them mI, which previous studies identify as one of the markers. For the purpose of this study, a more demanding policy for considering the validity of the spectra has been defined: only spectra with $0.8 < Cr3.9 < 1.2$ is going to be considered acceptable. By limiting the ratio of Cr3.9 to a 20% of its correct value (it is known that the ratio has to be 1), those spectra that had problems with water suppression or noise will be filtered, thus obtaining better definition of metabolite concentrations.

From the spectral data considered valid, the quality of the fit will be measured considering as valid only those concentrations with CRLB < 20%.

5.3 Results and Discussion

From the original 9 controls and 12 depressed patients, only 5 controls and 7 depressed patients produced acceptable spectra. The rest were filtered because they did not comply with $0.8 < Cr3.9 < 1.2$. The reason for that amount of spectra being filtered is not only the use of a more demanding policy for defining acceptable spectra, but also the fact that the

spectra was obtained from patients, not from volunteers, as was done in the previous studies. The scanning time for obtaining a JPRESS spectrum is 17 minutes, which imply that the patient will move, thus adding more noise to the MRS signal. In this particular study this problem was worsened by the fact that it focused on elderly patients.

Table VIII. Concentrations of metabolites using 3T JPRESS-ProFit for Controls (left) and Depressed patients (right).

	3 T 2D JPRESS-ProFit Controls			3 T 2D JPRESS-ProFit Depressed		
	% Valid	**Ratio/Cr**	**CRLB**	**% Valid**	**Ratio/Cr**	**CRLB**
Cr301	100	1±0	1.12±0.49	100	1±0	0.88±0.26
Cr391	100	0.9±0.09	2.26±1.12	100	1.07±0.08	1.48±0.49
NAA	100	0.95±0.24	4.49±4.56	100	1.21±0.29	1.71±0.82
GPC	80	0.2±0.09	9.95±7.79	85	0.26±0.03	4.96±1.25
PCh	60	0.19±0.12	15.4±7.02	15	0.28±0	9.58±0
Cho	20	0.05±0	10±0	15	0.04±0	10±0
Ala	60	0.18±0.12	10.93±5.65	42	0.09±0.03	13.15±5.12
Asp	60	0.37±0.06	9.32±5.43	85	0.48±0.11	6.68±0.64
GABA	60	0.25±0.09	9.16±5.9	85	0.43±0.14	4.54±0.91
Glc	80	0.52±0.13	6.42±3.18	100	0.64±0.18	5.53±3.55
Gln	60	0.26±0.11	11.3±1.15	100	0.35±0.12	8.74±2.17
Glu	100	0.99±0.14	4.54±2.62	100	1.22±0.15	2.75±0.57
Gly	60	0.11±0.05	16.36±1.51	57	0.07±0.02	13.97±3.86
GSH	100	0.31±0.04	4.33±2.2	100	0.32±0.02	3.28±0.85
Lac	80	0.25±0.09	8.03±4.21	85	0.14±0.06	8.39±1.99
mI	100	0.96±0.21	3.5±2.14	100	1.3±0.13	2.01±0.79
NAAG	40	0.49±0.21	3.9±0.61	71	0.29±0.16	8.00±7.4
PE	80	0.47±0.1	6.68±2.73	85	0.56±0.11	4.59±1.26
Tau	0	-	-	28	0.28±0.26	11.5±4.94
Scy	60	0.09±0.03	7.11±4	85	0.06±0.04	8.5±4.15
Asc	100	0.57±0.17	6.18±5.64	100	0.72±0.06	3.06±0.68
NAA+NAAG	100	1.18±0.46	1.22±0.67	100	1.46±0.16	0.6±0.19
GPC+PCh+Cho	100	0.31±0.04	1.18±0.28	100	0.29±0.03	1.6±0.21
Gln+Glu	100	1.18±0.28	4.35±2.79	100	1.6±0.21	2.43±0.49

Table VIII presents the results of this pilot study. From the values obtained, Cho and Tau did not reach 40% of valid quantitations so they will not be considered for the study. Considering the rest of the metabolites, the results are in agreement with the previous 1D

and 2D results reported in the literature: an increase in mI, PE, and Glx for depressed patients. In this study, mI goes from 0.96 in controls to 1.3 in depressed patients, PE goes from 0.47 in controls to 0.57 in depressed patients and Glx (Gln+Glu) go from 1.18 in controls to 1.6 in patients. Figure 21 compares the concentrations obtained. Nevertheless, in this study, the difference was statistically meaningful for mI with $p<0.01$ and for Glx (Gln+Glu) with $p<0.05$, although it was not statistically meaningful for PE. As for the rest of the metabolites, although there are differences, for example NAA is higher in depressed patients (1.21) that in controls (1.09), those differences are not statistically meaningful except for Glu. Glu increases in depressed patients, going from 0.99 in controls to 1.22, and the difference is statistically meaningful with $p<0.05$. This result was expected as Glu was one of the components of Glx.

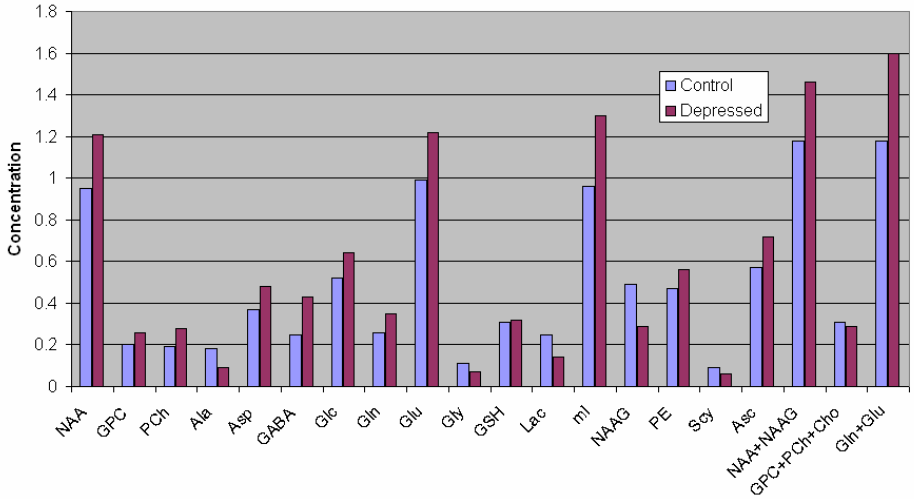

Figure 21. Comparison of metabolite concentrations between Control and Depressed patients.

5.4 Conclusions

This chapter has presented an example of how ProFit in combination with 2D spectroscopy can be applied to clinical studies. The example used, the characterization of

late life depression patients, has already been studied in the literature using 1D and 2D spectroscopy. The results obtained confirm the state of the art, but identify two metabolites for which the difference in concentration is statistically meaningful, mI and Glu/Glx, thus identifying possible markers.

One of the main conclusions of this example should be the importance of the definition of a policy for determining which spectral data is going to be considered in the study. The requisites suggested by ProFit, although valid when working with volunteers, can not be applied to clinical studies. For these cases, because the goal is the identification of statistically meaningful markers, the data considered for the study should be carefully selected. As a consequence of implementing a more demanding policy more data will be discharged. This increase is also caused by the fact that the data is obtained from patients, which in general will have a very different behavior from volunteers. So far, due to the time required to acquire the spectra, a repetition of the measurement in a clinical environment is not possible.

The goal of this study was not to find markers for late life depression, but to give an example of how metabolite quantitation can be very useful for characterizing clinical pathologies. For confirming the results presented here more data needs to be acquired and processed.

CHAPTER 6

CONCLUSIONS AND FUTURE WORK

Although the potential of MRS in clinical problems has been recognized long time ago, it has not become a completely routine clinical procedure, mainly because of the complexity of the process. The main goal of this thesis was to further investigate tools and give reasons for the use of spectroscopy in clinical applications.

This thesis has focused in three main areas: (1) Implementation and further optimization of a recently developed algorithm (ProFit) to process the 2D JPRESS data acquired at UCLA Radiology using Siemens 3T and 1.5T MRI scanners; (2) Modification of the ProFit algorithm to process the 2D L-COSY data acquired using Siemens 3T and 1.5T MRI scanners; and (3) Pilot evaluation of the 2D JPRESS-based ProFit algorithm in a small group of patients diagnosed with late life depression.

Regarding the first two topics, ProFit has been adapted to work with the 2D JPRESS and COSY data acquired using the Siemens 3T and 1.5T MRI scanners, and prior knowledge has been generated for processing brain data and phantom data. The preliminary results indicate that: (1) 3T provides higher quality results that 1.5T; (2) 2D spectroscopy provides more dependable and accurate results than 1D and (3) COSY provides better quality results that JPRESS.

The clinical example provided in the last chapter indicates how straight forward and useful the application of 2D MRS quantitation is for clinical applications and highlights the importance of selecting the data for the study.

As for future works, there are different lines that look promising:

- Application of 2D spectroscopy for characterization of prostate patients with cancer or BPH (Benign Prostate Hyperplasia). The application of metabolite quantitation to this area is not as straight forward as it may seems due to the complexity of obtaining quality spectra from the prostate.
- In a clinical environment, one of the problems that 2D spectroscopy faces is its time requirements. One area that looks promising for reducing the total acquisition time is covariance NMR.
- Although the earlier ProFit developer claims that spectra are processed on average in 1 minute, our experience shows that this is an optimistic approximation. In general average processing time for JPRESS is 10 minutes and for COSY up to 35 minutes. If quantitation wants to be used in clinical environments this processing time has to be reduced. New fitting techniques can be implemented for reducing processing time.
- ProFit implementation does not offer a graphical interface that can be used for processing the data. Currently, the processing of spectral data is highly dependent on the operator's knowledge about the algorithm and the running environment (Matlab). A graphical interface would help to introduce 2D spectroscopy and its quantitation to clinical environments. This idea is valid, in general, for all quantitation environments which, up to know, require an operator that has some technical knowledge of the algorithm.

REFERENCES

[1] Antoine, J.P., Chauvin, C., Coron. A. Wavelets and related time-frequency techniques in magnetic resonance spectroscopy. NMR Biomed 14, 2001.

[2] Bartholdi, E., Ernst R.R. Fourier spectroscopy and the causality principle. J. Magn. Reson. 11: 9-19, 1973.

[3] Binesh, N., Kumar, A., Hwang, S., Mintz, J., Thomas, M.A. Neurochemistry of Late-Lide Depression: A Pilot Two-Dimensional MR Spectrocopic Study. Journal of Magnetic Resonance Imaging 20: 1039-1045, 2004.

[4] Bolan P.J., BelaBarre, L., Baker, E.H., Merkel, H., Everson, L.I., Yee, D., Garwood, M. Eliminating spurious lipid sidebands in 1H MRS of breast lesions. Magn. Reson. Med. 48:215-222, 2002.

[5] Bottomley, P.A. Spatial localization in NMR spectroscopy in vivo. Ann. N. Y. Acad. Sci. 508: 333-48, 1987.

[6] Cavassila, S., Deval, S., Huegen, C., van Ormondt, D., Graveron-Demilly, D. Cramer-Rao Bound Expressions for Parametric Estimation of Overlapping Peaks: Influence of Prior Knowledge. Journal of Magnetic Resonance 143, 311-320, 2000.

[7] Cavassila, S., Deval, S., Huegen, C., van Ormondt, D., Graveron-Demilly, D. Cramer-Rao bounds: an evaluation tool for quantitation. NMR Biomed 14: 278-283, 2001.

[8] Chong V.H.F., Rumpel, H., Aw, Y., Ho, G., Fan, Y., Chua, E. Temporal lobe necrosis following radiation therapy for nasopharnygneal carcinoma: ^{1}H spectroscopic findings. Int. J. Radiat. Oncol. Biol. Physics 45: 699-705, 1999.

[9] Chung, H. Multiple Quantum and Multi-Dimensional MR Spectroscopy in Human Tissue in-vivo. Ph.D. Thesis, University of California, Los Angeles, 2003.

[10] de Beer, R., van Ormondt, D., Pijnapel, W.W.F. Quantification of 1-D and 2-D magnetic resonance time domain signals. Pure Appl. Chem. 64: 815-823, 1992.

[11] Delikatny, E.J., Hull, W.E., Mountford, C.E. The effect of altering time domains and window functions in two-dimensions proton COSY spectra of biological specimens. J. Mag. Reson. 94: 563-573, 1991.

[12] GAMMA, http://gamma.ethz.ch/

[13] Govindaraju, V., Young, K., Maudsley, A.A. Proton NMR chemical shifts and coupling constants for brain metabolites. NMR Biomed. 13:129-153, 2000.

[14] http://sermn02.uab.cat/mrui/

[15] Hurd, R., Sailasuta, N., Srinivasan, R., Vigneron, D.B., Pelletier, D., Nelson, S.J. Measurement of brain glutamate using TE-averaged PRESS at 3T. Magn Reson. Med. 51: 435-440, 2004.

[16] Kreis, R., Boesch, C. Spatially localized, one and two-dimensional NMR spectroscopy in vivo application to human muscle. J. Magn. Reson. B 113:103-118, 1996.

[17] Kumar, A., Thomas, M.A., Lavretsky, H., Yue, K. et al. Frontal White Matter Biochemical Abnormalities in Late-Life Depression Detected with Proton Magnetic Resonance Spectrocopy. Am. J. Psychiatry 159:4, 2002.

[18] LC-Model Webpage. http://s-provencher.com/pages/lcmodel.shtml.

[19] Metzger, G.J., Patel, M., Hu, X. Applications of genetic algorithms to spectral quantification. J. Magn. Reson. Ser. B 110: 316-320, 1996.

[20] Meyer, R.A., Fisher, M.J., Nelson, S.J. Evaluation of manual methods for integration of in vivo phosphorus NMR Spectra. NMR Biomed 1(3): 131-135, 1998.

[21] Miersova, S., Ala-Korpela, M. MR spectroscopy quantitation: a review of frequency domain methods. NMR Biomed 14, 2001.

[22] Miller, M.I., Greene, A.S. Maximum Likelihood estimation for nuclear magnetic resonance spectroscopy. Journal of Magnetic Resonance 83: 525-548, 1989.

[23] Provencher, S. Automatic quantitation of localizes in vivo spectra with LC-Model. NMR Biomed 14, 2001.

[24] Rose, S.E., de Zubicaray G.I., Wang. D., Galloway, G.J., Chalk, J.B., Eagle, S.C., Semple, J., Doddrell, D.M. A ^{1}H MRS study of probable Alzheimer's disease and normal aging: implications for longitudinal monitoring of dementia progression. Magn. Reson. Imaging 17:291-299, 1999.

[25] Savic, I., Lekvall, A., Greitz, D., Helms, G. MR spectroscopy shows reduced frontal lobe concentrations on N-acetyl aspartate in patients with juvenile myoclonic epilepsy. Epilepsia 41: 290-296, 2000.

[26] Schulte, R., Lange, T., Beck, J., Meier, D., Boesiger, P. Improved two-dimensional J-resolved spectroscopy. NMR Biomed; 19: 264-270, 2006.

[27] Schulte, R.F., Boesiger, P. ProFit: two-dimensional prior-knowledge fitting of J-resolved spectra. NMR Biomed 19: 255-263, 2006.

[28] Slotboom, J., Hofman, L., Boesch, C., Kreis, R. Two-dimensional fitting with prior knowledge constraints: the solution for glutamate/glutamine quantitation at 1.5T?. Proc. 7th Annual Meeting of ISMRM, 1561-1569, 1999.

[29] Smith, S.A., Levante, T.O., Meier, B.H., Ernst, R.R. Computer Simulations in Magnetic Resonance. An Object Oriented Programming Approach. J. Magn. Reson., 106a, 75-105, 1994.

[30] Stanley, J.A., Drost, D.J., Williamson, P.C., Thomson, R.T. The use of a priori knowledge to quantify short echo *in vivo* ^{1}H MR spectra. Magn. Reson. Med. 34: 17-24, 1995.

[31] Stoyanova, R., Brown, T.R. NMR spectral quantitation by principal component analysis. NMR Biomed 14, 2001.

[32] Thomas MA, Binesh N, Yue K, DeBruhl N. Volume-localized two-dimensional correlated magnetic resonance spectroscopy of human breast cancer. J Magn Reson Imaging 14(2):181-6, 2001.

[33] Thomas, M., Binesh, N., Yue, K., Banakar, S., Wyckoff, N., Huda, A., Marumoto, A., Raman, S. Adding a new spectral dimension to localized ^{1}H MR spectroscopy of human prostates using an endorectal coil. First International Conference on Biomedical Spectroscopy: From molecules to men, Cardiff, UK, 7-10 July 2002.

[34] Thomas, M.A., Hattori, N., Umeda, M., Sawada, T., Naruse, S. Evaluation of two dimensional L-COSY and JPRESS using a 3T MRI scanner: from phantoms to human brain in vivo. NMR Biomed 16:245-251, 2003.

[35] Thomas, M.A., Hattori, N., Umeda, M., Sawada, T., Naruse, S. Evaluation of two-dimensional L-COSY and JPRESS using a 3t MRI scanner: from phantoms to human brain in vivo. NMR in Biomedicine 16: 245-251, 2003.

[36] Thomas, M.A., Yue, K., Binesh, N., Davanzo, P., Kumar, A., Siegel, B. et al. Localized Two-Dimensional Shift Correlated MR Spectrocopy of Human Brain. Magnetic Resonance in Medicine 46:58-67, 2001.

[37] van den Boogaart, A., Howe, F.A., Rodrigues, L.M., Stubbs, M., Griffiths, J.R. *In vivo* ^{1}P MRS: absolute concentrations, signal-to-noise and prior knowledge. NMR Biomed. 8: 87-93, 1995.

[38] van der Veen, J.W.C., de Beer, R., Luuyten, P.R., van Ormondt, D. Accurate quantification of in vivo P NMR signals using the variable projection method and prior knowledge. Journal of Magnetic Resonance 6, 92-98, 1988.

[39] Van hecke, P., Van Huffel, S. Editorial: NMR spectroscopy quantitation. NMR Biomed 14:223, 2001.

[40] Vanhamme, L., Sundin, T., Van Hecke, P., Huffel, V. MR spectroscopy quantitation: a review of time-domain methods. NMR Biomed 14:233-246, 2001.

[41] Vanhamme, L., van der Boogaart, A., van Huffel, S. Improved method for accurate and efficient quantification of MRS data with use of prior knowledge. Journal of Magnetic resonance 129, 35-43, 1997.

[42] Weber, O.M., DUc, C.O., Meier, D., Boesiger, P. Heuristic optimization algorithms applied to quantification of spectroscopic data. Magn Reson. Med. 39: 723-730, 1998.

[43] Young, K., Khetselius, D., Soher, B.J., Maudsley, A.A. Confidence Imgaes for MR Spectrocopic Imaging. Magnetic Resonance in Medicine 44:537-545, 2000.

[44] Yue, K., Marumoto, A., Binesh, N., Thomas, M.A. 2D JPRESS of human prostates using an endorectal receiver coil. Mag. Reson. Med. 47: 1059-1064, 2002.

[45] Zandt, H.J.A., Van de Graaf, M., Heerschap, A. Common Processing of in vivo MR spectra. NMR Biomed 14, 2001.